CHIRAL MODELS: PIONS AND BARYONS*

M. PRASZAŁOWICZ

Institute of Physics, Jagellonian University,
Reymonta 4, 30-059 Cracow, Poland

(Received May 30, 1991)

Various aspects of chiral models are discussed with special emphasis on the chiral quark model and the Skyrme model. Firstly, the ability of the chiral quark model to reproduce pion scattering data is reviewed. Secondly the soliton sector of the model is studied. The soliton solution is interpreted as a baryon — nucleon or dilambda. Next, on the example of the Skyrme, model we study inclusion of strangeness, large N_c limit and quantization. It is argued that effective chiral models qualitatively reproduce the low energy limit of QCD.

PACS numbers: 11.30.Rd; 12.40.Aa; 14.20.-c

1. Introduction

Quantum Chromodynamics (QCD), the ultimate theory of strong interactions, is not directly applicable at low energies, where conventional perturbation theory ceases to be valid. The only way to implement QCD in this energy regime is to use lattice formulation and computer simulations. However it is just this energy range, where the full complexity of the nonabelian gauge theory plays an essential role, requiring larger and larger lattices, dedicated computers and more computer time. An alternative approach consists in constructing so-called *effective* models and studying their properties. Thus, while it is a very tall order to *derive* such models from QCD, we can at least use some of the symmetries or approximate symmetries of QCD to construct phenomenological Lagrangians relevant to low energy physics. QCD with (almost) massless quarks has a *chiral* symmetry and any sensible approximation to QCD must respect this symmetry.

* Thesis submitted to the Jagellonian University, Department of Physics, in partial fulfilment of the requirement for the habilitation degree

In this paper we discuss a wide class of effective low energy models which are based on chiral symmetry. They are commonly called *chiral models.* Rather than giving a complete review, we try to formulate a clear physical picture, with its highlights as well as limitations, which accommodates two important aspects of low energy particle physics: pion scattering and baryon properties. This work summarizes author's contributions already published in journals [1–9] (although some of the results presented in Sections 3 and 4 are new) and as such covers only those topics which were of direct interest to him. Although exhaustive reviews can be found in the literature [10–16], the attempt is here to make this work to large extent self-contained.

Low energy effective models describing pions and nucleons were discussed well before the advent of QCD. The mediators of strong interactions: gluons, as well as quark matter fields, are not directly observable. It is well known that at large distances QCD becomes a confining theory, and only color singlet states, such as pions, appear in nature. Ideally, we should like to start with a theory defined by the QCD Lagrangian and by some series of operations recast it into a form involving pions and perhaps baryons [17–21]. In two space-time dimensions such bosonisation indeed takes place; in four dimensions, however, bosonisation is by no means obvious.

In Section 2 we will argue that one can formally *integrate out* gluons from the QCD Lagrangian [22–27]. The resulting nonlocal quark theory [27] would, however, respect chiral symmetry [23, 24]. One can approximate this very complicated and, as yet, quite unknown theory by a simple, chirally symmetric, quartic quark interactions. A model with such properties was formulated by Nambu and Jona-Lasinio [28], however in a different context. This model exhibits an important phenomenon: spontaneous chiral symmetry breaking. It turns out that, for certain model parameters, originally massless fermions acquire a nonzero mass. Moreover, a massless quark-antiquark bound state emerges – the pion. Formally, one can now reexpress the interaction part of the Nambu – Jona-Lasinio Lagrangian introducing an auxiliary, composite pion field. We will call this model the chiral quark model (χQM). Let us stress here that at this stage the introduction of auxiliary pion fields is merely a question of convenience and elegance.

The identical low-momenta Lagrangian [20, 21] has been recently discussed within the instanton picture of the QCD vacuum [20, 21, 29, 30]. Thanks to a numerically small "diluteness" parameter found from instanton dynamics, all collective excitations of the vacuum can be, theoretically speaking, divided into two classes [21]: those whose masses tend to zero with the packing fraction of instantons, and those whose masses remain constant. The effective Lagrangian contains both kinds of excitations, however of more interest to us is the part where only the light degrees of freedom

are present, with the second class of excitations, such as scalar mesons or η', frozen out.

The remaining light degrees of freedom are now described by a remarkably simple χQM-type theory involving only quarks with a momentum-dependent dynamical mass $M(k)$, interacting with the pseudo-Goldstone chiral field. Since the momentum dependence of $M(k)$ is characterized also by a relatively large typical scale [4–6], one can freeze $M(k)$ at zero momentum. Though numerically $M(0) = 345$ MeV [20, 21] is not much smaller than, say], the η' mass (957 MeV), their ratio is theoretically small in the packing fraction of instantons. It can be further diminished by slightly heating QCD (with chiral symmetry still broken) [31]. Then the quark-pion theory becomes "more" exact.

What is important and what distinguishes our approach from those of Refs [32–39], where similar quark-pion effective Lagrangians were considered, is the absence of explicit kinetic energy or, say, Skyrme-type [40, 41] terms for the pion field: they arise only from quark loops when one integrates out the quark fields. This means that pions are, in fact, composite fields. Ideologically it is a welcome feature in comparison with models where pions are actually point-like, whereas in Nature the nucleon and the pion have the same size. This is exactly what one gets from χQM: both particles appear to have radii of the order of $1/M$ (the pion charge radius has been calculated in Ref.[20]). The absence of local pion counterterms also solves the vacuum instability paradox [38, 39] (for a discussion see Refs [22, 42]).

The chiral quark model requires an ultraviolet regularization, which in the case of the instanton motivated version of the model is in fact provided naturally by the rapid falloff of the dynamical quark mass $M(k)$. In this paper, however, we shall use a more practical regularization in the proper time [43] representation for quark loops (for details see in Appendix A).

In Section 2 we examine the ability of the chiral quark model to reproduce pion-pion scattering data [8]. It is certainly important to know whether the model, which we will eventually use to describe baryons, is compatible with pion physics in the first place. Employing a gradient expansion [44–46], we derive an effective Lagrangian involving only pion fields, and calculate scattering amplitudes up to the sixth order in the pion momenta [26, 47, 48]. Keeping in mind the astonishing simplicity of the model we conclude that the χQM model reproduces pion partial waves with satisfactory accuracy. We discuss the limitations of the model due to the cutoff always present in an effective theory such as χQM.

The essential new element of χQM in comparison with other quark models is that the same Lagrangian which describes low energy pion scattering also describes baryons, via the classical *soliton* solution [6, 40–42, 49–55]. Assuming that the classical pion field takes a special, spherically

symmetric configuration, we study the spectrum of the Dirac Hamiltonian in the presence of such a configuration and develop techniques to sum up the contribution of the Dirac see — vacuum polarization. We observe that the vacuum energy *increases* almost linearly with a suitably defined size of the pion-soliton field. At the same time a valence level, with three (or N_c) quarks emerges from upper continuum. Its energy *decreases* with the soliton size. The sum of the two contributions: valence + sea develops a stable minimum which we interpret as a *classical* baryon.

We also examine another form of a classical Ansatz for the chiral pion field based on an SO(3) embedding in the SU(3) flavor group [56, 57]. This configuration corresponds to a dilambda (or H) dibaryon state [58]. Indeed, unlike in the nucleon case, two valence levels with six (or $2N_c$) quarks appear [7]. The existence of such a state is still not confirmed experimentally [59]. It naturally emerges, however, in other models of the baryon such as, *e.g.* the M.I.T. bag [58].

Numerically our results fall into a *within* 20 % category. In Section 3 we thoroughly formulate the soliton problem within the framework of χQM and discuss numerics. Our results, however, deal with the classical soliton configurations only. In order to account for Δ — N splitting for example, one has to quantize the model. The quantization consists in rotating the soliton solution and in introducing the generalized coordinates and momenta. Although qualitatively the result of this procedure is known: one obtains the Hamiltonian of the quantum-mechanical rotator. Quantitatively one has to find moments of inertia of the rotating soliton — which is a fairly complicated exercise. Some work in this direction is already in progress [60].

In order to envisage the full structure of the quantized model, in Section 4 we discuss the Skyrme model [40, 41], which, in a sense, appears as a limiting case of χQM for large soliton size [21]. Historically of course the Skyrme model was formulated well before even the invention of the quark. It was however abandoned for more than 20 years until Witten suggested that QCD could in fact give rise to solitonic configurations of the chiral field, which would have a nonzero baryon number [61–63]. Here an important assumption was made: the baryon number was identified with a topological number of the chiral field [64, 65].

In Section 4 we review the Skyrme model phenomenology in a simple approach, where all relevant quantities can be calculated analytically. We discuss SU(3) baryon and dibaryon phenomenology, chiral symmetry breaking due to large strange quark mass and the large N_c limit [66, 67] of the model. All these problems are in fact present in χQM as well, therefore our analysis of Section 4, although interesting by itself, may constitute a starting point for technically more involved studies in the chiral quark model.

There are many points we do not discuss or even touch upon in this

work. Certainly one can calculate other baryon properties such as magnetic moments, form-factors, weak decay amplitudes *etc.* [3, 4, 13, 68]. One can consider more complicated effective actions involving vector mesons or higher derivative couplings for example [69–71]. One can also construct different classical solutions corresponding for instance to pion condensate, [72, 73] many-baryon states or deuteron. These problems were either discussed by other authors or work on them is still in progress. We briefly return to these problems in Section 5 where we also summarize our findings and provide conclusions.

2. Chiral Lagrangians and chiral quark model

The Euclidean generating functional of QCD reads (*e.g.* [21]):

$$Z_{\rm QCD} = \int [D\psi][D\psi^\dagger] \exp\left(i \int d^4x\, \psi^\dagger(\not\partial + m)\psi\right) \int [DA] \exp\left(i \int d^4x \left(g\psi^\dagger \not A \psi + \tfrac{1}{4} F \cdot F\right)\right), \qquad (2.1)$$

where the small bare mass matrix m for quarks has been introduced. Here ψ denotes the quark field, A — the gluon field and F is the gluon field strength. At low energies, however, neither quarks nor gluons are the relevant observed degrees of freedom. Instead, we have almost massless pions, slightly heavier kaons and η, and heavy baryons. Is there a way to reexpress Eq. (2.1) in terms of these physical degrees of freedom ?

Formally this task has not been achieved owing to enormous technical difficulties [19, 22]. One can however imagine the following scenario: first integrate out the gluons [23, 24]. The resulting action would then describe the nonlinear and nonlocal many quark interactions [27]. The next step would consist in linearizing this complicated action and expressing it in terms of local color singlet composite fields corresponding to pseudo-scalar, vector and tensor mesons coupled in a chirally invariant way to quark fields ψ. At first approximation only pseudo-scalars (= Goldstone bosons) would contribute [74] and we would be left with a quark-pion effective theory. Finally, we would have to integrate out quarks to end up with the pion (or π–K–η) effective Lagrangian [22, 25, 75, 76]. So, we go through the following chain of effective actions:

$$S_{\rm QCD}[\psi, A] \to S^{\psi}_{\rm eff}[\psi] \to S_{\chi{\rm QM}}[\psi, \pi] \to S^{\pi}_{\rm eff}[\pi], \qquad (2.2)$$

where χQM stands for the chiral quark model.

It should be kept in mind that the arrows in Eq. (2.2) do not indicate a rigorous derivation of one action from another but rather *educated guesses*

based mainly on symmetry principles and some physical input. Various choices for the actions in chain (2.2) have been contemplated in literature. We shall first discuss the most general action S^{π}_{eff} and its relevance to $\pi - \pi$ scattering [77–81]. Then we will show that one of the simplest choices for $S_{\chi\text{QM}}$ is in good agreement with the data for pion-pion scattering.

The purpose of the analysis in this Section is threefold: first we want to show that χQM is compatible with the pion scattering data, second — we will show that the gradient expansion works well for pion scattering and third — we will stress the importance of a cutoff in an effective theory like χQM. Although the model is not supposed to work at energies above the ρ resonance it is certainly interesting to see how the tail of the ρ resonance builds up in the gradient expansion. The model also predicts a new non-zero partial wave of $J = 3$ and $I = 1$, which is, however, quite small: it arises at the 6-th order of the gradient expansion.

2.1. π - π scattering

In this Section our discussion will be confined to the case of two flavors. QCD with two almost massless quarks has a chiral SU(2) symmetry which is spontaneously broken, with pions emerging as the Goldstone bosons [77]. The interactions of these bosons have been successfully described by the Lagrangian:

$$L_2 = \frac{F_\pi^2}{16}\mathrm{Tr}\left(\partial_\mu \overline{U}\partial^\mu \overline{U}^\dagger\right) + \frac{m_\pi^2 F_\pi^2}{16}\mathrm{Tr}\left(\overline{U} + \overline{U}^\dagger\right), \tag{2.3}$$

where matrix

$$\overline{U} = \exp\left(i\frac{2\vec{\tau}\cdot\vec{\pi}}{F_\pi}\right) \tag{2.4}$$

transforms under the chiral SU(2) group as

$$\overline{U} \to L\,\overline{U}\,R^\dagger. \tag{2.5}$$

(In our notation pion decay constant is equal $F_\pi = 186$ MeV.)

In spite of the phenomenological success, Lagrangian (2.3) contains no information specific to QCD. A systematic approach to calculate low energy amplitudes consists of constructing chiral Lagrangians with more than two derivatives [78, 79]. In this way the effective action S^{π}_{eff} can be constructed. For example at the next order the most general Lagrangian for massless pions is given by:

$$L_4 = \frac{\alpha_1}{4}\left(\mathrm{Tr}\left(\partial_\mu \overline{U}\partial^\mu \overline{U}^\dagger\right)\right)^2 + \frac{\alpha_2}{4}\mathrm{Tr}\left(\partial_\mu \overline{U}\partial_\nu \overline{U}^\dagger\right)\mathrm{Tr}\left(\partial^\mu \overline{U}\partial^\nu \overline{U}^\dagger\right). \tag{2.6}$$

The form of these two terms is dictated by the chiral symmetry alone; however, unlike in the case of L_2, the coefficients α_1 and α_2 are free parameters and should be found by dynamical considerations. In the next section we will show how they can be computed in a chiral quark model.

We do not intend to make a general analysis of the all possible Lagrangians with six derivatives. We shall rather content ourselves with the specific Lagrangian $L_6^{\chi QM}$ which can be derived from the χQM [26, 47, 48]. Below we enlist those terms of $L_6^{\chi QM}$ which contain four pion fields [8]:

$$\begin{aligned}\overline{L}_6 = &\ \beta_1 (\partial_\mu \vec{\pi} \cdot \partial^\mu \partial_\rho \vec{\pi})(\partial_\nu \vec{\pi} \cdot \partial^\nu \partial^\rho \vec{\pi}) \\ &+ \beta_2 (\partial_\mu \vec{\pi} \cdot \partial^\mu \vec{\pi})(\partial_\nu \partial_\rho \vec{\pi} \cdot \partial^\nu \partial^\rho \vec{\pi}) \\ &+ \beta_3 (\partial_\mu \vec{\pi} \cdot \partial_\nu \partial_\rho \vec{\pi})(\partial^\nu \vec{\pi} \cdot \partial^\mu \partial^\rho \vec{\pi}) \\ &+ \beta_4 (\partial_\mu \vec{\pi} \cdot \partial_\nu \partial_\rho \vec{\pi})(\partial^\mu \vec{\pi} \cdot \partial^\nu \partial^\rho \vec{\pi}) \\ &+ \beta_5 (\partial_\mu \vec{\pi} \cdot \partial_\nu \vec{\pi})(\partial^\mu \partial_\rho \vec{\pi} \cdot \partial^\nu \partial^\rho \vec{\pi}). \end{aligned} \tag{2.7}$$

Lagrangians (2.3, 2.6) and (2.7) generate amplitudes for the process:

$$\pi_a(p_a) + \pi_b(p_b) \to \pi_c(p_c) + \pi_d(p_d) \tag{2.8}$$

in terms of a single function $A(s,t,u)$ [81], where the Mandelstam variables are defined as:

$$s = (p_a + p_b)^2, \quad t = (p_a - p_c)^2, \quad u = (p_a - p_d)^2. \tag{2.9}$$

The amplitude for the process (2.8) is defined as:

$$T_{abcd} = A(s,t,u)\,\delta_{ab}\delta_{cd} + A(t,s,u)\,\delta_{ac}\delta_{bd} + A(u,t,s)\,\delta_{ad}\delta_{bc}. \tag{2.10}$$

The amplitudes with definite isospin are given by:

$$\begin{aligned} T^0(s,t,u) &= 3A(s,t,u) + A(t,s,u) + A(u,t,s), \\ T^1(s,t,u) &= A(t,s,u) - A(u,t,s), \\ T^0(s,t,u) &= A(t,s,u) + A(u,t,s) \end{aligned} \tag{2.11}$$

and, from these, one can project out the partial waves:

$$T_l^I = \frac{1}{64\pi} \int_{-1}^{1} d\cos\theta\, P_l(\cos\theta) T^I(s,t,u). \tag{2.12}$$

Functions $A_i(s,t,u)$ corresponding to the Lagrangians L_2, L_4 and $\overline{L}_6$ can be now straightforwardly computed [8, 80]:

$$A_2(s,t,u) = \frac{4}{F_\pi^2}(s - m_\pi^2), \tag{2.13}$$

$$A_4(s,t,u) = \frac{8}{F_\pi^4}\left(4\alpha_1\left(s - 2m_\pi^2\right)^2 + \alpha_2\left(s^2 + (t-u)^2\right)\right), \tag{2.14}$$

$$\begin{aligned} A_6(s,t,u) = {} & \tfrac{1}{2}\beta_1\, s\left(s - m_\pi^2\right)^2 \\ & - \beta_2\left(s - 2m_\pi^2\right)^3 \\ & + \tfrac{1}{2}\beta_3\, s\left(t - 2m_\pi^2\right)\left(u - 2m_\pi^2\right) \\ & - \tfrac{1}{2}\beta_4\left(\left(u - 2m_\pi^2\right)^3 + \left(t - 2m_\pi^2\right)^3\right) \\ & - \tfrac{1}{2}\beta_5\left(s - 2m_\pi^2\right)\left(\left(u - 2m_\pi^2\right)^2 + \left(t - 2m_\pi^2\right)^2\right). \end{aligned} \tag{2.15}$$

2.2. Chiral quark model

In this Section we shall concentrate on the chiral quark model. Let us start by specifying the lagrangian which describes the interactions of pions with two light quarks represented by an isospinor ψ [8]:

$$L_{\chi\mathrm{QM}} = \overline{\psi}\left(i\partial\!\!\!/ - M\overline{U}^5 - \epsilon\,\overline{U}^5 \partial\!\!\!/\, \overline{U}^5 - m\right)\psi, \tag{2.16}$$

where

$$\overline{U}^5 = \overline{U}\,\frac{1+\gamma_5}{2} + \overline{U}^\dagger\,\frac{1-\gamma_5}{2}, \tag{2.17}$$

M denotes a constituent quark mass, m stands for the bare (or current) quark mass matrix and

$$\epsilon = \tfrac{1}{2}(1 - g_A). \tag{2.18}$$

Here a remark concerning the *quark* axial coupling g_A is in order. In the simplest version of χQM $g_A = 1$. However Manohar and Georgi [82] argued that since at low energies there is only a vector symmetry, g_A can be, in principle, renormalized away from 1. Following their discussion, where they claim that $g_A \approx 0.75$, we have introduced the $\epsilon = (1 - g_A)/2$ piece in the Lagrangian of Eq. (2.16). There is also a phenomenological reason to introduce $g_A \neq 1$; namely, the *nucleon* axial coupling G_A calculated in the chiral quark model with $g_A = 1$ is usually smaller than its experimental value, $G_A = 1.23$.

At this point we should also quote recent paper by Weinberg [83]. Weinberg argues that the effective quarks should have $g_A = 1, 0$ or -1. Only the first choice is physically plausible. We leave aside here the question whether g_A can or cannot be different from 1 and proceed to the derivation of the effective pion action. In what follows, unless stated otherwise, we will assume that $M \approx 345$ MeV and $\overline{m} \approx 5.5$ MeV [84].

Let us now formally integrate out the quarks. The result is of course well known: one gets a determinant of the Dirac operator defined in Eq. (2.16), which can be recast in the form of an effective action:

$$S^{\pi}_{\text{eff}}[\pi] = \frac{N_c}{2} \log \text{Sp}\left(\frac{D^{\dagger}D}{D_0^{\dagger}D_0}\right), \tag{2.19}$$

where Sp denotes a functional trace as well as a matrix trace over spinor and isospin indices. D is the Dirac operator of Eq. (2.16) and D_0 is the same operator but with $\overline{U} \equiv 1$.

In fact S^{π}_{eff} of Eq. (2.19) is defined as the *real* part of the pion effective action [49]. The *imaginary* part can be in principle also computed [21, 85] — it corresponds to the anomalous piece — however in the case of two flavors this anomalous part vanishes identically [62, 63].

Expression (2.19) is divergent and must be regularized. In this paper we use the *proper time* regularization [43]:

$$S^{\text{reg}}_{\text{eff}}[\pi] = -\frac{N_c}{2}\int_0^{\infty}\frac{d\tau}{\tau}\varphi(\tau)\,e^{-\tau} \text{Sp}\left(\exp\left(-\tau\,\frac{D^{\dagger}D}{M^2}\right) - \exp\left(-\tau\,\frac{D_0^{\dagger}D_0}{M^2}\right)\right) \tag{2.20}$$

with step-like cutoff function $\varphi(\tau)$.

Although finite, effective action $S^{\text{reg}}_{\text{eff}}$ is a nonlocal functional of the field $\overline{U}$. One way to handle such functionals is to expand them in powers of $\partial\overline{U}$. We have used heat kernel techniques [44–46] to recast $S^{\text{reg}}_{\text{eff}}$ into the form of effective Lagrangians (2.3, 2.6, 2.7). Comparing the first two terms of this expansion (see Appendix A) with L_2 we get two constraints on the function $\varphi(\tau)$ for $g_A = 1$:

$$\frac{N_c M^2}{\pi^2}\int_0^{\infty}\frac{d\tau}{\tau}\varphi(\tau)e^{-\tau} = F_{\pi}^2, \tag{2.21}$$

$$\frac{N_c M^2}{4\pi^3}\int_0^{\infty}\frac{d\tau}{\tau^2}\varphi(\tau)e^{-\tau} = \frac{m_{\pi}^2 F_{\pi}^2}{2\overline{m}} = -\langle\overline{\psi}\psi\rangle, \tag{2.22}$$

where $\overline{m}$ is an average u and d quark mass, and the quark condensate is [21]

$$-\langle\overline{\psi}\psi\rangle = (249\ \mathrm{MeV})^3.$$

In Ref. [6] it was shown that for $M = 345$ MeV and $\overline{m} = 5.5$ MeV the above conditions are satisfied by a simple step-like function:

$$\varphi(\tau) = \frac{1}{1+(\frac{0.643}{\tau})^{1.3}\mathrm{e}^{-2.2\tau}}. \tag{2.23}$$

For $g_A \neq 1$ Eq. (2.21) takes the following form [8]:

$$\begin{aligned}\Phi_0 &\equiv \int_0^\infty \frac{d\tau}{\tau}\varphi(\tau)\mathrm{e}^{-\tau} \\ &= \frac{\pi^2 F_\pi^2}{N_c g_A^2 M^2}\end{aligned} \tag{2.24}$$

and, if we go to the next order, i.e. to four derivatives of $\overline{U}$ we get:

$$\begin{aligned}\alpha_1 &= -\frac{N_c}{8\pi^2}\left(\frac{\Phi_0}{12}\left(1-g_A^2\right)^2 + \frac{\Phi_1}{6}g_A^2\left(2-3g_A^2\right) + \frac{\Phi_2}{4}g_A^4\right), \\ \alpha_2 &= \frac{N_c}{8\pi^2}\left(\frac{\Phi_0}{12}\left(1-g_A^2\right)^2 + \frac{\Phi_1}{3}g_A^2\left(1-g_A^2\right) + \frac{\Phi_2}{6}g_A^4\right).\end{aligned} \tag{2.25}$$

Cutoff dependent coefficients

$$\Phi_{k+1} = \frac{1}{k!}\int_0^\infty d\tau\,\tau^k\varphi(\tau)\,\mathrm{e}^{-\tau} \tag{2.26}$$

tend to 1 when cutoff is removed (*i.e.* $\varphi(\tau) \equiv 1$). Formula (2.26) can be extended to negative k by assuming that $(-|k|)! \equiv 1$.

At the order $(\partial\overline{U})^6$ we get [8]:

$$\begin{aligned}&\beta_1 = \overline{\Phi}_3\left(\frac{4\Phi_2}{5\Phi_3} - 1\right), && \beta_2 = -2\overline{\Phi}_3, \\ &\beta_3 = \tfrac{4}{5}\overline{\Phi}_3, && \beta_4 = \tfrac{8}{5}\overline{\Phi}_3, \\ &\beta_5 = \tfrac{8}{5}\overline{\Phi}_3, && \text{with}\quad \overline{\Phi}_3 = \frac{N_c}{96\pi^2 F_\pi^4 M^2}\Phi_3\end{aligned} \tag{2.27}$$

for $g_A = 1$. As earlier stated we do not intend to make the general analysis of the six-order terms, rather we shall content ourselves with qualitative

analysis of the radius of convergence of the derivative expansion given in terms of L_2, L_4 and $\overline{L}_6$ for the case of $g_A = 1$.

Let us first analyze how sensitive to the choice of g_A are the fourth order coefficients α_1 and α_2 given by Eq. (2.25). Instead of taking any specific form for the function $\varphi(\tau)$, like Eq. (2.23), we have found that for *all* choices for $\varphi(\tau)$ we have tried: $0.7 < \Phi_1 < 1$ and $0.92 < \Phi_2 < 1$. In Fig. 1 we plot the band of uncertainty for both α_1 and α_2 arising from varying Φ_1 and Φ_2 within the above limits. It can be seen that in fact for g_A not too small the fourth order coefficients are not very sensitive to the precise value of g_A. From now on we will assume that $g_A = 1$.

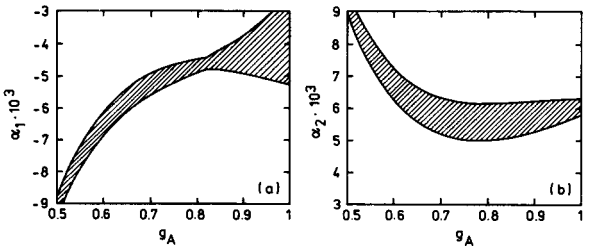

Fig. 1. Allowable range for parameters α_1 and α_2 as functions of g_A. The shaded area corresponds to the variations of the cutoff function φ , as described in the text

We wish to compare the scattering amplitudes calculated from the tree level effective Lagrangians $L_2 + L_4 + \overline{L}_6$ with the experimental data. Although these amplitudes are in general complex our results are necessarily real (we do not include boson loops) and therefore violate unitarity. In most cases, however, the imaginary parts generated by the pion loops are small in the energy region below 700 MeV. Only for T_0^0 the lowest order tree-level amplitude violates unitarity at about 550 MeV.

On the other hand the data have large errors; there is also some systematical dicrepancy between various experiments. The best tree-level fit to all existing partial waves done with 4-order Lagrangian L_4 gives [80]:

$$\alpha_1 = -0.0092, \qquad \alpha_2 = 0.0080, \tag{2.28}$$

whereas χQM predicts [8]:

$$\alpha_1 = -0.0044, \qquad \alpha_2 = 0.0058, \tag{2.29}$$

where the cutoff function of Eq. (2.23) was used. The two results are contradictory; it is therefore useful to plot them against the experimental data. In Fig. 2 we plot χQM predictions for the real parts of the $\pi - \pi$ scattering amplitudes. We do not plot the best fit amplitudes; they are in general

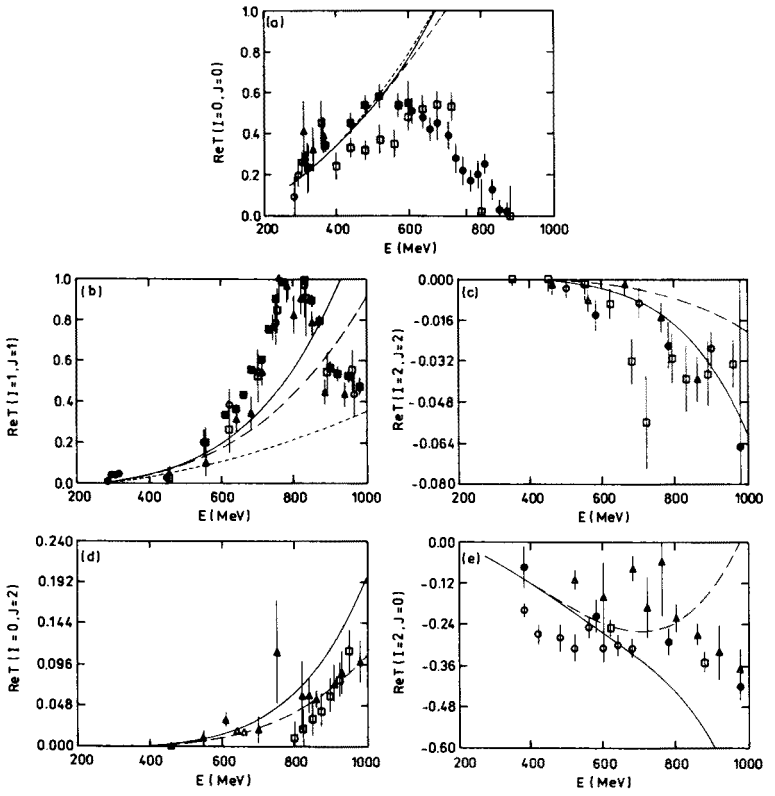

Fig. 2. Tree-level $\pi - \pi$ scattering amplitudes for χQM. Short dashed line corresponds to the lowest order (2 derivative) amplitude, for long dashed line we have added 4 derivative terms and the solid line represents full result with 6 order terms included. The data were compiled by J.F. Donoghue in Ref.[80] (see also [8])

not much different for the scattering energies below 500 MeV. The most pronounced difference is of course for $\mathrm{Re}T_0^0$, where the best fit turns down starting from $E = 550$ MeV following the data points [8]. In Fig. 2 we also plot amplitudes with the 6-order terms included.

The purpose of these comparisons was threefold. Firstly we have shown that χQM is consistent with $\pi - \pi$ scattering amplitudes. This consistency was questioned in the literature [86]; our results do not support this criticism. Also recent calculations of $\gamma\gamma \to \pi^0\pi^0$ and $\mathrm{K_L} \to \pi^0\gamma\gamma$ in χQM do agree with the data [87]. The result of Ref. [76] shows that the generalized SU(3) χQM produces the effective Lagrangian which agrees with the phenomenological parametrization of Gaser and Leutwyler [78, 79]. This makes us confident that χQM is a good starting-point for investigating the soliton solutions which we would like to interpret as baryons.

Secondly, it is an interesting issue to see whether the gradient expansion works for pion scattering. In most cases the 6-order terms are small in comparison with the amplitudes obtained from both L_2 and L_4. The 4-order terms always correct the second-order Weinberg formula in the right direction. On the other hand one may be surprised that the fits presented on Fig. 2 are consistent with the data up to energies of the order $E \sim 2.5M$. After all, M sets the scale for the gradient expansion and one would naturally expect that it should break down for energies of the order of M. There is, however, another energy scale in the problem, namely the cutoff. It is often assumed in the literature that the cutoff should be removed from finite quantities *i.e.* from Φ_k for $k > 0$. Within the present accuracy of the experimental data it is hard to argue whether the amplitudes calculated with the cutoff are substantially better than those without; however one should always remember that the cutoff is present in an effective theory such as χQM. This cutoff, Λ, as we shall discuss in detail in the next Section, is of the order of 600 – 800 MeV, and therefore the model predictions are in fact confined to the energy range below Λ. The constituent mass M and the cutoff Λ are not independent; they are related through the constraint condition (2.21) — this may offer an explanation why the gradient expansion works so well up to 800 MeV.

3.Solitons in the chiral quark model

In this Section we will describe how baryons emerge in a model based on the lagrangian density of Eq. (2.16). In the $N_c \to \infty$ limit N_c quarks inside a nucleon can be considered as a classical source for the pion field. The nucleon problem in this limit appears to be similar to that of a large Z atom, allowing a semiclassical Thomas–Fermi treatment [6, 49]. One has to minimize the aggregate energy of the quark Dirac sea in a trial pion field, plus the energy of N_c quarks bound on a discrete level (see Fig. 3). The trial pion field which minimizes this quantity is called, after Thomas–Fermi, the self-consistent pion field. In what follows we will assume that this self-consistent pion field takes the form of *hedgehog* (or *soliton*) configuration.

In the remaining part of this Section we will show that there exist non-trivial quark-meson configurations, which we interpret as baryons, for a constituent quark mass $M > 300$ MeV. For $M > 400$ MeV these configurations have energies below the free quark threshold. The above values become modified if we change the quark-meson axial coupling g_A, however the qualitative picture remains unchanged. Our results basically agree with those obtained by means of different calculational procedures presented in Refs [50–55]. We also calculate the value of the σ term [6] and find that $\sigma = 55$ MeV, in agreement with recent phenomenological analysis [88, 89].

We also consider another *soliton* solution [7] based on SO(3) embedding in the SU(3) group [56, 57] interpreting it as a dilambda (or H particle). Since 1977, when Jaffe showed that within the framework of the M.I.T. bag model a six quark state (uuddss - called H) has mass as low as 2150 MeV [58] there have been many calculations of the H mass in various models (bag model [90, 91], lattice QCD [92, 93],quark cluster model [94, 95] and Skyrme model [56, 57, 96, 97]) with predictions ranging from 1.56 GeV to above 3 GeV. If $M_H < 2M_\Lambda$ then H would be stable with respect to strong interactions and could be seen in forthcoming experiments [59]. Therefore it is of considerable importance to have a reliable prediction for its mass.

Employing, the so-called *two-point* approximation we find that $M_H = 2.11$ GeV in the chiral limit [7]. The singlet part of the mass operator shifts this value by less than $\Delta M = 300$ MeV in a surprising coincidence with the naive expectation: $\Delta M = 2m_s$, where m_s denotes the strange quark mass [7].

Results presented in this Section deal in fact with the classical nucleon. By rotating the hedgehog-like pion field (3.6) we can account for nucleon-delta splitting [49, 60]. Quantities such as the relevant moments of inertia or magnetic moments, etc., require the knowledge of quark wave functions. This interesting, but quite complicated analysis for the baryon octet and decuplet remains to be carried out. In the next Section we will discuss the quantization of the rotational zero modes using the Skyrme model as an example.

3.1. Dirac equation and soliton energy

In this Section we discuss the basic tools used to calculate the soliton mass. In the next Sections we will use these methods to calculate the nucleon and dilambda masses. We are looking for a minimum of the functional:

$$M_{\rm sol}[\overline{U}] = \min\left(N_c E_{\rm level}[\overline{U}] + E_{\rm field}[\overline{U}]\right), \tag{3.1}$$

where $E_{\rm level}[\overline{U}]$ is the energy of a bound state level which emerges from the upper Dirac continuum when the trial pion field is switched on, and $E_{\rm field}[\overline{U}]$ is the total energy of the Dirac sea including the possible discrete levels coming up from lower or upper continuums in the same trial pseudoscalar field, with the free (*i.e.* with $\overline{U} = 1$) Dirac sea energy subtracted (see Fig. 3):

$$E_{\rm field}[\overline{U}] = N_c \sum_n (E_n - E_n^0). \tag{3.2}$$

In fact the sum in Eq. (3.2) has to be regularized. The sum extends over all levels in upper and lower continuum (the *symmetric* case) or only over lower continuum (*asymmetric* case) – see Appendix B for details.

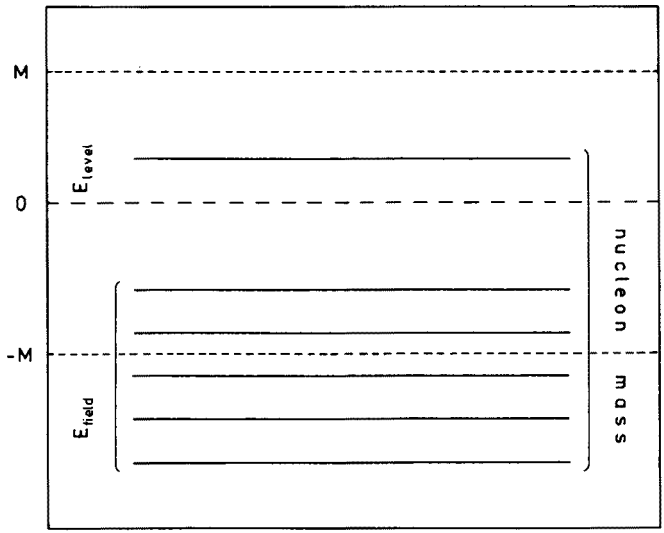

Fig. 3. The spectrum of the Hamiltonian (3.3) in the presence of the pseudoscalar field. Solid lines denote occupied levels. Nucleon mass M_N is calculated by summing the energies of the occupied levels (minus the energy of the corresponding levels with the pion field switched off)

The Dirac Hamiltonian determining the spectrum is given by:

$$H = \gamma_0 \left(\gamma_k \frac{\partial}{\partial x_k} + M \overline{U}^5 + \epsilon \overline{U}^5 \gamma_k \frac{\partial \overline{U}^5}{\partial x_k} + m \right). \tag{3.3}$$

This Hamiltonian commutes neither with the isospin operator $\mathbf{T}$ nor with the total angular momentum operator $\mathbf{J} = \mathbf{L} + \mathbf{S}$, but only with their sum, the so called *grand spin*, $\mathbf{K} = \mathbf{T} + \mathbf{J}$.

As explained in Appendix B (see also Ref. [6]) the quantity E_{field} can be expressed in terms of the phase shifts of the Dirac equation corresponding to Hamiltonian (3.3). We will use two expressions for E_{field}, *symmetric*:

$$\begin{aligned} E_{\text{field}}^{\text{sym}} = & \frac{N_c}{2} \sum_{K,\lambda} (2K+1) \\ & \left(- \int_M^{\infty} dE \, \frac{dF}{dE} \, \frac{\delta^{K,\lambda}(E)}{\pi} + \int_{-M}^{-\infty} dE \, \frac{dF}{dE} \, \frac{\delta^{K,\lambda}(E)}{\pi} \right. \\ & \left. + \sum_{\text{up}} \left(F(E_n^{K,\lambda}) - F(M) \right) + \sum_{\text{low}} \left(F(E_n^{K,\lambda}) - F(-M) \right) \right), \end{aligned} \tag{3.4}$$

or *asymmetric*:

$$E_{\text{field}}^{\text{asym}} = N_c \sum_{K,\lambda} (2K+1) \left(\int_{-M}^{-\infty} dE \, \frac{dF}{dE} \, \frac{\delta^{K,\lambda}(E)}{\pi} + \sum_{\text{low}} \left(F(E_n^{K,\lambda}) - F(-M) \right) \right). \quad (3.5)$$

Here K denotes grand spin, λ other quantum numbers, like parity for instance, and n enumerates discrete levels of given K and λ which emerged from a given continuum.

Due to the theorem $\mathrm{Sp}(H - H_0) = 0$ both expressions (3.5) and (3.6) should be equal for the suitably large cutoff. However, for constituent masses M comparable to the cutoff they can be, and as we shall see they indeed are, different.

3.2. Nucleon in the chiral quark model

In this Section we calculate the soliton mass corresponding to the *time-independent* SU(2) symmetric (so called *hedgehog*) Ansatz proposed by Skyrme [40, 41]:

$$U_0 = \exp\left(i\vec{n} \cdot \vec{\tau} P(r) \right), \quad (3.6)$$

where $\vec{\tau}$ are isospin Pauli matrices, $\vec{n}$ is a unit a radial vector and P is a function of radial distance only. Instead of solving self-consistently equations of motion in order to find $P(r)$ which minimizes the energy (3.1), we take a variational approach and assume that $P(r)$ takes the following form:

$$P(r) = 2 \arctan\left(\left(\frac{r_0}{r} \right)^2 \right). \quad (3.7)$$

Here r_0 — the soliton size — is the variational parameter and the second power of r_0/r is determined by the long distance behaviour of the equations of motion. More complicated family of three parameter Ansätz for P were considered in Ref. [6].

In order to diagonalize the Dirac equation we take the quark isospinor-bispinor wave function in the form

$$\psi_{K K_3}(\vec{r}) = \frac{1}{r} \begin{bmatrix} -i F(r) \, \Sigma_{K,K_3}^{(-,-)}(\vec{n}) - i J(r) \, \Sigma_{K,K_3}^{(+,+)}(\vec{n}) \\ G(r) \, \Sigma_{K,K_3}^{(-,+)}(\vec{n}) - H(r) \, \Sigma_{K,K_3}^{(+,-)}(\vec{n}) \end{bmatrix}, \quad (3.8)$$

where spinor-isospinors $\Sigma_{K,K_3}^{(i,j)}(\vec{n})$ can be found in Appendix C. Note that K takes integer values. The Dirac eigenvalue equation

$$H \, \psi_{K K_3}(\vec{r}) = E \, \psi_{K K_3}(\vec{r}) \quad (3.9)$$

for given K and K_3 comes to a system of four ordinary differential equations for scalar functions F, G, H and J (see Appendix C). The parity of the solution (3.8) and hence of the equation (3.9) is equal to $\mathrm{P} = (-1)^{K+1}$. The solutions corresponding to parity $\mathrm{P} = (-1)^K$ are obtained by exchanging the rows of the isospinor-bispinor (3.8). The case $K = 0$ is special: functions F and G have to be put equal to zero in Eq. (3.8). In this way the four equations (3.9) reduce to a system of two differential equations for scalar functions H and J.

When we continuously vary the pion field by increasing r_0, the energy levels in upper an lower continuums are shifted with respect to their position with the pion field switched off. For the pion field strong enough some of the continuum levels my turn into the discrete ones, as depicted schematically in Fig. 3. In Fig. 4 the energy of the discrete levels for $K = 0$ and $K = 1$ are plotted as functions of r_0. The $K = 0$ sector is somewhat special: only here some levels which originated from the upper continuum may cross the $E = 0$ line to disappear in the lower continuum as $r_0 \to \infty$. The number of such levels is equal to the topological charge of the pion field [21, 49]. Indeed, in Fig. 4.a only one level crosses the $E = 0$ line.

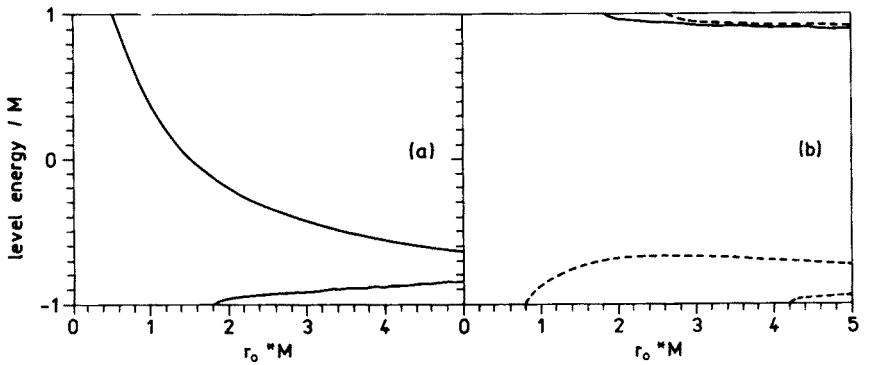

Fig. 4. Energy of discrete levels of the Hamiltonian (3.3) as a function of variational parameter r_0 for $K = 0$ (a) and $K = 1$ (b); solid line corresponds to parity $+1$, dashed to parity -1

To find the phase shifts for the $K \neq 0$ sector the following procedure is applied [6]. The system (3.9) has two solutions regular at $r = 0$. Let us denote them by superscript $i = 1, 2$. They behave at the origin as:

$$\begin{aligned} F^{(1)}(r) &= O(r^K); & G^{(1)}(r) &= O(r^{K+1}); \\ H^{(1)}(0) &\equiv 0; & J^{(1)}(0) &\equiv 0; \\ H^{(2)}(r) &= O(r^{K+1}); & J^{(2)}(r) &= O(r^{K+2}); \\ F^{(2)}(0) &\equiv 0; & G^{(2)}(0) &\equiv 0 \end{aligned} \qquad (3.10)$$

and at large distances:

$$\begin{aligned} F^{(i)}(r) &= A^{(i)} \sin\left(kr + \alpha^{(i)}\right), \\ G^{(i)}(r) &= A^{(i)} \frac{k}{E+M} \cos\left(kr + \alpha^{(i)}\right), \\ H^{(i)}(r) &= B^{(i)} \sin\left(kr + \beta^{(i)}\right), \\ J^{(i)}(r) &= B^{(i)} \frac{k}{E+M} \cos\left(kr + \beta^{(i)}\right) \end{aligned} \tag{3.11}$$

with $k = \sqrt{E^2 - M^2}$, where $A^{(i)}$, $B^{(i)}$, $\alpha^{(i)}$ and $\beta^{(i)}$ are found by solving numerically Eq. (3.9). The phase shift δ for given K is then defined as [6, 49]:

$$\tan\delta = \frac{A^{(1)}B^{(2)} \cos(\alpha^{(1)} + \beta^{(2)}) - A^{(2)}B^{(1)} \cos(\alpha^{(2)} + \beta^{(1)})}{A^{(1)}B^{(2)} \sin(\alpha^{(1)} + \beta^{(2)}) - A^{(2)}B^{(1)} \sin(\alpha^{(2)} + \beta^{(1)})}. \tag{3.12}$$

The possible bound states are found from the condition:

$$A^{(1)}B^{(2)} - A^{(2)}B^{(1)} = 0, \tag{3.13}$$

where this time $A^{(i)}$ and $B^{(i)}$ are the coefficients in front of the exponentially decaying solutions with the initial conditions given by Eqs (3.10).

In Figs 5 and 6 we plot the energy behaviour of the phase shifts $\delta(E)$ for $K = 0$ sector. For comparison the full line represents a semiclassical approximation to $\delta(E)$ given by the formula:

$$\begin{aligned} \frac{\delta(E)}{\pi} = \epsilon\,\mathrm{sign}(E) + \frac{1}{2|E|\pi} \int_0^\infty dr \Big(& 2\frac{\sin P}{r}\left(M + \epsilon\frac{\sin P}{r}\right)(1-2\epsilon) \\ & + \epsilon\,(2\sin 2P + \epsilon P' r)\frac{P'}{r}\Big) + O\left(\frac{1}{E^2}\right). \end{aligned} \tag{3.14}$$

The derivative coupling proportional to ϵ forces the phase shifts to approach a constant $\pm\pi\epsilon$ as E tends to infinity. This behavior is clearly seen in Figs 5 and 6. Moreover for upper continuum and parity $+1$ $\delta(E = M)$ jumps from 0 to π between $r_0M = 0.3$ and $r_0M = 0.8$. This is an illustration of the Levinson Theorem stating that $\delta(E = M)/\pi$ counts the number of discrete levels which emerged from a given continuum (see Appendix B). Indeed, a valence level emerges from the upper continuum at $r_0M \approx 0.5$.

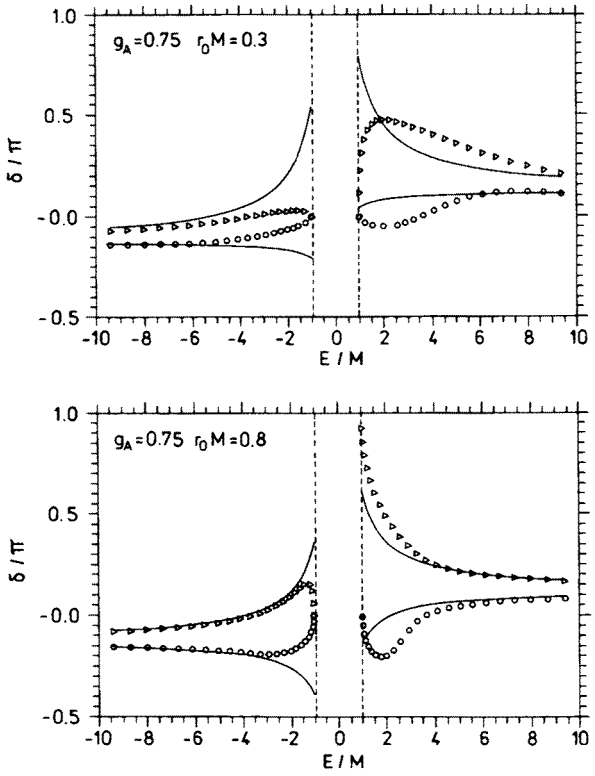

Fig. 5. Phase shifts for $K = 0$, triangles for parity P$= +1$, squares for parity P$= -1$ for different r_0M and $g_A = 0.75$. Solid curves correspond to the semiclassical asymptotics of Eq.(3.14)

Since for $m = 0$ everything scales with M the plots of Fig. 6 are exactly the same for any value of the constituent mass M.

Having found the energy behavior of the phase shifts in a given K sector by means of Eq. (3.12) we perform the integration according to Eq. (3.5) or Eq. (3.6) (the integral is convergent owing to the presence of the regularization factors $F'(E)$), add a possible discrete level found by means of Eq. (3.13), and repeat this procedure for the opposite parity. What remains, is to perform the summation over K. One does not need to go to infinitely large K with the described procedure. The behavior of large K partial waves is semiclassical (since it implies large orbital quantum number). A simple formula can be derived to estimate their contribution to E_{field} :

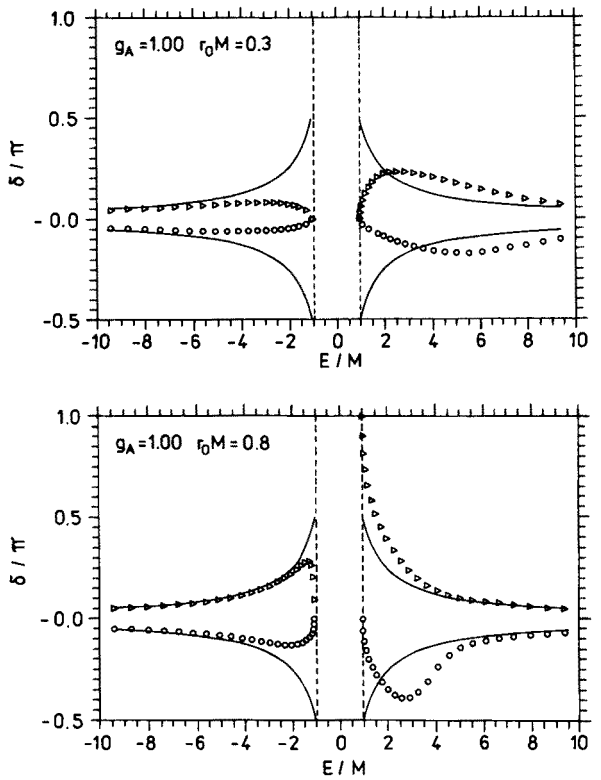

Fig. 6. Phase shifts for $K = 0$, triangles for parity P$= +1$, squares for parity P$= -1$ for different r_0M and $g_A = 1$. Solid curves correspond to the semiclassical asymptotics of Eq.(3.14)

$$E^K_{\text{class}} \equiv \sum_\lambda E^{K,\lambda}_{\text{class}} \approx \frac{N_c M^2}{2} \int_0^\infty \frac{dt}{\sqrt{\pi t}} \varphi(tM^2) e^{-tM^2} \int_0^\infty dr\, r \exp\left(-\frac{r^2}{2t}\right) I_{K+\frac{1}{2}}\left(\frac{r^2}{2t}\right)\left(P'^2 + 2\frac{\sin^2 P}{r^2}\right). \quad (3.15)$$

Here $I_{K+1/2}$ is the modified Bessel function, and λ stands for parity P. Summing up E^K_{class} over K with the multiplicity factor $(2K + 1)$ one gets the long wavelength limit given by the first term of Eq.(A.12), namely:

$$E_{\text{class}} = \frac{N_c M^2}{2\pi} \int_0^\infty \frac{dt}{t} \varphi(tM^2)\, e^{-tM^2} \int_0^\infty dr\, r^2 \left(P'^2 + 2\frac{\sin^2 P}{r^2}\right). \quad (3.16)$$

In order to calculate the energy of the Dirac sea we have used the following identity:

$$E_{\text{field}} = E_{\text{class}} - \sum_{K=0}^{K_{\max}} \left(E^K_{\text{class}} - E^K_{\text{field}} \right), \tag{3.17}$$

which is by definition true in the limit $K_{\max} = \infty$ (the quantities E^K_{field} are calculated numerically in terms of the phase shifts). In practice good numerical accuracy is obtained for $K_{\max} = 3$.

In the previous Section we have specified the cutoff function φ (Eq. (2.23)) which satisfies the conditions (2.21) and (2.22). In fact the cutoff dependence is very weak [9], therefore in the present calculations we have used the so-called *sharp* cutoff:

$$\varphi(\tau) = \Theta(\tau - \tau_0), \tag{3.18}$$

where τ_0 was chosen to satisfy constraint (2.21) and then $\overline{m}$ was adjusted to fulfil Eq. (2.22).

The existence of a nontrivial solution which has interpretation of a nucleon manifests itself as a minimum of $E \equiv M_{\text{sol}}$ as a function of the variational parameter r_0. In Fig. 7 we plot E/M as a function of a dimensionless parameter $r_0 M$ for different masses M and couplings g_A. For $g_A = 1$ the minimum appears for $M > 300$ MeV and gets deeper as M increases. For $M > 400$ MeV the minimum is achieved at $E < 3M$, *i.e.* below the free quark threshold. The minimum appears because of two competing phenomena: the *increase* of the sea energy, E_{field} with r_0 and the rapid *decrease* of the energy of the valence level emerging from the upper continuum. This pattern can also be seen for $g_A = 0.75$.

Soliton mass is a decreasing function of the constituent quark mass M. For $g_A = 1$ the minimum appears for $M \approx 325$ MeV at approximately $E \approx 1190$ MeV to reach 1060 MeV for $M = 500$ MeV. For $M > 600$ MeV the valence level crosses the $E = 0$ line and the soliton consists of the sea only. This limit corresponds to the Skyrme model, where there are no quarks but the pseudoscalar field only. Here a remark concerning the cutoff is in order. For $M = 325$ MeV the energy cutoff $\Lambda = M/\sqrt{\tau_0}$ is of the order of 665 MeV, whereas for $M = 500$ MeV, $\Lambda = 645$ MeV. It is clear that model makes sense only when $M < \Lambda$, so we cannot increase the constituent mass M too far. The above numbers are calculated by means of the *asymmetric* mass formula (3.6). For $M \approx 300 - 400$ MeV both formulae (3.6) and (3.5) give results within a few percent, whereas for $M = 500$ MeV the difference is already larger than 100 MeV.

As seen from Fig. 7 the minima are rather broad; it is therefore difficult to estimate their exact positions, *i.e.* r_0, with high accuracy. Therefore the

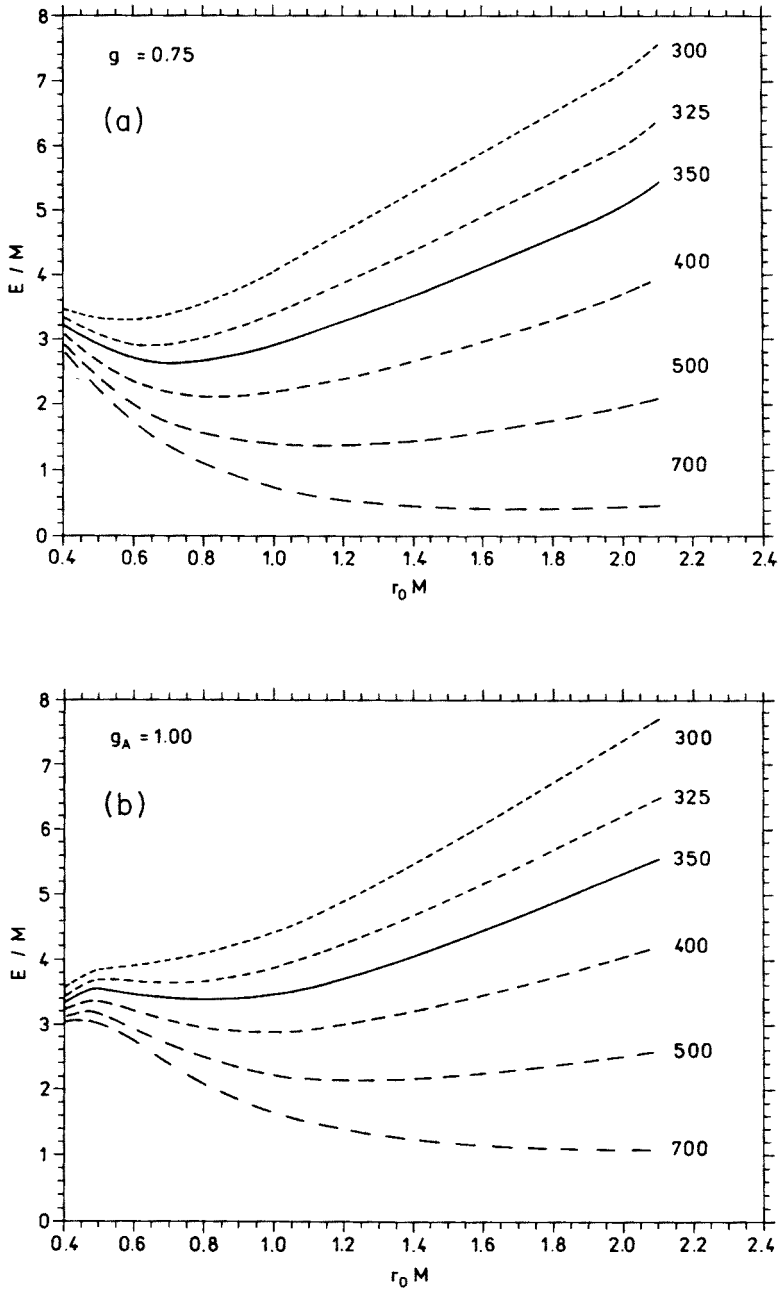

Fig. 7. Soliton energy (in units of M) dependence on r_0 for different constituent quark masses; (a) $g_A = 0.75$, (b) $g_A = 1$

nucleon axial coupling G_A, which is related to the long distance tail [98] of the profile function $P(r)$:

$$G_A = \frac{16\pi}{3} F_\pi^2 r_0^2 \tag{3.19}$$

has larger relative errors than the soliton energy inself. Typical values of G_A are 0.5 to 0.9 for $M = 325 - 500$ MeV respectively. The model fails to reproduce experimental value for $G_A = 1.23$

So far we have concentrated our attention on the chiral limit *i.e.* on a theory with massless quarks. It is interesting to look at the slope of the bare quark mass dependence of the soliton mass $E(m)$. This slope is just a nucleon "σ-term" [99]:

$$\sigma = \overline{m}\langle \text{nucleon}|\bar{u}u + \bar{d}d|\text{nucleon}\rangle. \tag{3.20}$$

where $\overline{m} = 5.5$ MeV is an average up- and down-quark mass. By definition the nucleon matrix element in Eq. (3.20) is evaluated in the chiral limit. To compare Eq. (3.20) with the data one needs to calculate the corrections generated by the quark masses. They have been estimated in Ref. [88] to be of the order of 5 MeV (see also Ref. [89]. Experimental results are also subject to uncertainties due to the extrapolation of the data to the Cheng-Dashen point [89]. The analysis of Koch [100, 101] gives 64 ± 8 MeV, whereas Gasser *et al.* [89] quote slightly lower value: 56 ± 2MeV which correspond to theoretical $\sigma = 59$ MeV or $\sigma = 51$MeV respectively. So large σ term implies a large content of strange pairs in nucleon [102, 103]. It is quite easy to calculate the σ-term in our model:

$$\sigma = m\frac{\partial}{\partial m} E\Big|_{m=0}. \tag{3.21}$$

To calculate (3.21) we have used the cutoff function of Eq. (2.23) and $M = 345$ MeV as dictated by the model of the instanton vacuum. Our result reads [6]

$$\sigma = 54 \text{ MeV}. \tag{3.22}$$

One should note that in calculating derivative (3.21) systematic errors cancel out. Therefore we consider this numerical estimate of the σ-term as quite reliable.

3.3. Dilambda in the chiral quark model

In this Section we calculate the mass of the H particle [7], a six quark, baryon number 2, SU(3) singlet state [58]. Working in the chiral limit we use the dynamical (constituent) quark mass $M = 345$ MeV as dictated by the instanton vacuum model. As in the case of the nucleon we will minimize

the soliton mass (3.1), however, instead of the SU(2) matrix $\overline{U}$ we will use, following Balachandran *et al.* [56, 57], the SU(3) matrix of the form:

$$U_{\rm H}(\vec{r}) = \exp\left(i\,\vec{n}\cdot\vec{\Lambda}\,f(r) + i\left((\vec{n}\cdot\vec{\Lambda})^2 - \tfrac{2}{3}\right)g(r)\right), \tag{3.23}$$

where $\vec{\Lambda} = (\lambda_2,\ \lambda_5,\ \lambda_7)$ and $\vec{n}$ is a unit vector. Matrices Λ_i generate an SO(3) subgroup of the SU(3) flavor group. Ansatz (3.23) can be conveniently rewritten in the following form [7]:

$$(U_{\rm H})_{kl} = {\rm e}^{i\frac{g}{3}}\left(\delta_{kl}\cos f + n_k n_l\left({\rm e}^{-ig} - \cos f\right) + \varepsilon_{klm}n_m\sin f\right). \tag{3.24}$$

Functions f and g depend only on the radial distance r and are chosen to obey boundary conditions [56, 57, 96]:

$$\begin{aligned} f(0) &= \pi \quad \text{and} \quad f(r\to\infty) = \frac{1}{r^2} \\ g(0) &= \pm\pi \quad \text{and} \quad g(r\to\infty) = \frac{1}{r^3}. \end{aligned} \tag{3.25}$$

The general solution to the Dirac equation (3.9) with Ansatz (3.24) and $g_{\rm A} = 1$ can be written as:

$$\psi_{K\,K_3}(\vec{r}) = \begin{bmatrix} \sum\limits_{lj} F_{(l,j)}(r)\,\Xi^{(l,j)}_{KK_3}(\vec{n}) \\ -i\sum\limits_{lj} G_{(l,j)}(r)\Xi^{(l,j)}_{KK_3}(\vec{n}) \end{bmatrix}, \tag{3.26}$$

where the flavor-spinors $\Xi^{(l,j)}_{KK_3}$ can be found in Appendix C. Inserting (3.26) into Eq. (3.9) we get 12 first-order differential equations for 12 radial functions $F_{(l,j)}(r)$ and $G_{(l,j)}(r)$ ($l = \pm, 0$ and $i = \pm$). In fact, for the valence $K = 1/2$ level, the system reduces to 8 equations ($l = -$ does not contribute), which are solved numerically. Let us remark here, that since $U_{\rm H}$ does not transform into itself under parity transformation, parity is *not* a good quantum number here, and – unlike in the nucleon case – the 12 (or 8) equations do not split into two subsets of 6 (or 4) differential equations.

In order to calculate $E_{\rm level}$ we solve the Dirac equation numerically. To calculate $E_{\rm field}$ we use the interpolation formula (A.14) derived in Appendix A, which for Ansatz $U_{\rm H}$ can be recast into the form of an integral over dp :

$$E^{\rm int}_{\rm field} = 8MN_{\rm c}\int\limits_0^\infty dp\,\mathcal{G}(p)\Big(3\,(I_1^2+I_2^2) + (I_3^2+I_4^2) + 2\,(I_5^2+I_6^2) + 2\,(I_1 I_3 + I_2 I_4)\Big). \tag{3.27}$$

The integrals $I_k(p)$ are given by:

$$I_1 = \int_0^\infty dr \left((\cos f \cos\frac{g}{3} - 1) pr \sin pr \right.$$
$$\left. + (\cos f \cos\frac{g}{3} - \cos\frac{2g}{3})(\cos pr - \frac{\sin pr}{pr}) \right),$$

$$I_2 = \int_0^\infty dr \left(\cos pr \frac{d}{dr} \left(r \cos f \sin\frac{g}{3} \right) \right.$$
$$\left. + \left(\cos f \cos\frac{g}{3} + \sin\frac{2g}{3} \right) (\cos pr - \frac{\sin pr}{pr}) \right),$$

$$I_3 = -\int_0^\infty dr \left(\sin pr + 3 \left(\cos pr - \frac{\sin pr}{pr} \right) \right) \left(\cos f \cos\frac{g}{3} - \cos\frac{2g}{3} \right),$$

$$I_4 = -\int_0^\infty dr \left(\cos pr \frac{d}{dr} r \left(\cos f \cos\frac{g}{3} + \sin\frac{2g}{3} \right) \right.$$
$$\left. + 3 \left(\cos f \sin\frac{g}{3} + \sin\frac{2g}{3} \right) \left(\cos pr - \frac{\sin pr}{pr} \right) \right),$$

$$I_5 = p \int_0^\infty dr \frac{\sin pr}{pr} \frac{d}{dr} \left(r^2 \sin f \cos\frac{g}{3} \right),$$

$$I_6 = \int_0^\infty dr \sin f \sin\frac{g}{3} (pr \cos pr - \sin pr). \tag{3.28}$$

Finally we choose functions f and g in the form:

$$f = 2 \arctan \left(\frac{r_f}{r} \right)^2 \qquad g = 2 \arctan \left(\frac{r_g}{r} \right)^3, \tag{3.29}$$

where r_f and r_g are variational parameters.

Our procedure consists in finding a minimum of Eq.(3.1) with respect to parameters r_f and r_g . Since for wide range of r_g a minimum in r_f corresponds to $Mr_f = 1.1$, we vary only r_g. In Fig. 8 we plot E_{level}, $E^{\text{int}}_{\text{field}}$ and M_{H} as functions of Mr_g. M_{H} exhibits a shallow minimum for $Mr_g = 1.3$ with

$$M_{\text{H}} = 2.11 \text{ GeV}. \tag{3.30}$$

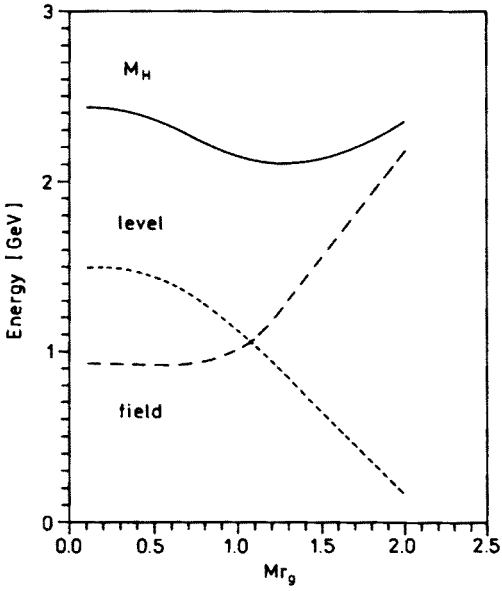

Fig. 8. E_{level}, $E^{\text{int}}_{\text{field}}$ and M_{H} as functions of variational parameter r_g, with $Mr_f = 1.1$

In order to depart from the chiral limit we have so far worked in, let us consider the quark mass matrix $m = \text{diag}(0, 0, m_s)$:

$$m = \tfrac{1}{3} m_s (1 - \sqrt{3}\,\lambda_8). \tag{3.31}$$

Since H is a flavor singlet only a piece proportional to 1 contributes to the H mass.

As we have seen in the previous Sections χQM is quite successful in reproducing the nucleon sigma term. In order to estimate the mass shift due to the singlet piece of the mass operator (3.31) we will calculate the dilambda σ-term in the chiral limit. One would naively expect that $\sigma_{\text{H}} = 2\sigma_{\text{N}}$, however our estimates based on the long wavelength expansion, Eq. (A.13), indicate that σ_{H} may be somewhat lower: $\sigma_{\text{H}} \approx 1.3\,\sigma_{\text{N}}$. The energy shift due to the singlet piece in (3.31) can be estimated in a linear approximation (for $m_s = 137$ MeV): $\Delta M_{\text{H}} = 580$ MeV. This large value suggests that the linear approximation is not applicable here and that nonlinearities in m_s should be taken into account. This can be achieved by minimizing M_{H} with m_s at its physical value. Note that the Ansatz functions (3.29) have to be modified, since they should decay exponentially at large r. The mass formula to be minimized now reads:

$$M_{\text{H}} = E_{\text{level}} + E^{\text{int}}_{\text{field}} + m_s \Delta,$$

where Δ is calculated from Eq. (A.13). Our estimate for $m_s = 137$ MeV indicates that $M_H \approx 2.4$ MeV at $Mr_g = 1.4$ and $Mr_f = 1.5$. This result coincides with the naive expectation $\Delta = 2$. Clearly, the nature of the SU(3) breaking in the soliton models is still an unsolved problem [104]. We relegate the detailed discussion of this point to the next Section where we discuss the SU(3) Skyrme model.

At this stage we are not in a position to decide whether M_H is below or above the two-Λ threshold. The model prediction for the mean octet mass [49, 60] gives 1207 MeV (exp. 1154 MeV), but splittings within the multiplets have not yet been evaluated. Let us finish by a remark that given a completely different group structure of the nucleon and dilambda Ansatze it is not obvious that SU(3) breaking can be treated in the same way in both cases.

4. Baryons in the SU(3) Skyrme model

In this Section we shall discuss the inclusion of strangeness using the Skyrme model as an example [11, 12]. Most of the problems encountered here are, however, inherent for the all chiral models [13]. The Skyrme model [40,41], because of its simplicity turns out to be a useful tool to address the question of the nature of chiral and SU(3) symmetry breaking due to the strange quark mass. For the sake of clarity we will use here the variational approach rather than exact numerical procedures. While our results differ by no more than 10 % from the exact ones found in the literature, most of the formulae in this work are analytical.

Let us briefly recapitulate the main ideas behind the Skyrme model. As we could see in Section 3.2, for large soliton sizes the valence level sinks in the Dirac sea. This means that the whole baryon mass can be expressed entirely in terms of parameters of the chiral field. It was Skyrme's idea that the soliton in the effective meson theory can be interpreted as the nucleon. Of course, this model was formulated well before the invention of quarks.

Skyrme proposed a specific effective Lagrangian involving the fourth power of the field derivatives (the Skyrme term) which guarantees stable solitonic solutions. When the model is quantized, this fourth order term involves, nevertheless, only second power of time derivatives [98]. The best fit fourth order coefficients of the effective chiral Lagrangian (see Eq. (2.28)) are consistent with Skyrme's conjecture. On the other hand, the effective Lagrangian obtained from χQM involves other terms (the non-Skyrme terms, see Eq. (A.12)), which destabilize the soliton and involve higher time derivatives in the quantum-mechanical treatment of the model. Unfortunately, as we saw in Section 2, we are not able to discriminate between the two effective Lagrangians, due to large experimental uncertainties.

Let us simply accept the original Lagrangian of Skyrme and proceed to a discussion of the Skyrme model phenomenology. We will assume that the chiral field U (which is an SU(3) generalization of the SU(2) $\overline{U}$ field) takes the form of a topological *hedgehog* configuration [63, 1]. We showed in Section 2 that the number of valence levels in χQM is equal to the topological charge of the chiral field. In the Skyrme model the baryonic current is, by assumption, identified with the conserved topological current [64, 65]. It is beyond the scope of this work to discuss the role of topology in detail; this question is widely covered in the literature [17,105]. Let us only mention that while in χQM one chooses the topological configuration merely for the sake of elegance and convenience (although it may happen that the topological field is selected by the dynamics [6]), in the Skyrme model the *hedgehog* configuration is absolutely necessary from the requirement of energy finiteness.

In this Section we cover a wide range of topics. First, we calculate the properties of the classical solution alone. Next we quantize the model [1, 106–108] and show that the system is constrained in such a way that the lowest energy states belong to octet and decuplet SU(3) representations. Treating the strange quark mass as a perturbation we discuss the baryon phenomenology [2, 107, 109, 110] as well as the properties of the H particle [96, 97]. The numerical results are not satisfactory. Finally, we discuss the large N_c limit [5, 111–113] and the "nonperturbative" approaches [114–118] in which the strange quark mass is not considered as a small parameter.

4.1. Classical solution

Let us start by specifying the effective Lagrangian proposed by Skyrme [40, 41] and later generalized by Witten [62, 63]:

$$\begin{aligned}\int dt\, L_{\mathrm{Sk}} = {} & \frac{F_\pi^2}{16}\int dt\, d^3r\, \mathrm{Tr}(\partial_\mu U^\dagger \partial^\mu U) \\ & + \frac{1}{32e^2}\int dt\, d^3r\, \mathrm{Tr}([\partial_\mu U\, U^\dagger, \partial_\nu U\, U^\dagger]^2) \\ & + N_c\, \Gamma_{\mathrm{WZ}} + \int dt\, L_m. \end{aligned} \tag{4.1}$$

Here U is an SU(3) matrix, N_c number of colors, parameters F_π and e, if taken from meson physics as discussed in Section 2, are equal to 186 MeV and $e \sim 5.5$ respectively.

The second term in Eq. (4.1) was proposed by Skyrme [40, 41] in order to stabilize the soliton. The third term (so called Wess-Zumino term [119, 120]) originates from topology [62]. It can be also derived from the CQM as the imaginary part of the action obtained by integrating out the quark fields

[85]. It accounts for chiral anomaly and cannot be written in terms of a local Lagrangian density; instead it is given as an integral over the 5-dimensional manifold whose boundary consists of 4-dimensional space-time:

$$\Gamma_{\rm WZ} = \frac{-i}{240\pi^2}\int d^5r\,\epsilon^{\mu\nu\rho\sigma\tau}\,{\rm Tr}\,(\partial_\mu U\,U^\dagger\partial_\nu U\,U^\dagger\partial_\rho U\,U^\dagger\partial_\sigma U\,U^\dagger\partial_\tau U\,U^\dagger). \quad (4.2)$$

In fact, as we shall see later explicitly, the fifth, redundant coordinate can be integrated out for the hedgehog Ansatz.

Last term in Eq. (4.1) explicitly breaks down chiral symmetry:

$$L_m = a\int d^3r\,{\rm Tr}\,(U + U^\dagger - 2) + b\int d^3r\,{\rm Tr}\,((U + U^\dagger)\lambda_8), \quad (4.3)$$

where a and b are given by:

$$a = \frac{F_\pi^2}{32}(m_\pi^2 + m_\eta^2), \quad b = \frac{\sqrt{3}F_\pi^2}{24}(m_\pi^2 - m_K^2). \quad (4.4)$$

Three pseudoscalar meson masses can be therefore expressed in terms of only two parameters yielding a constraint:

$$m_\pi^2 + 3m_\eta^2 - 4m_K^2 = 0, \quad (4.5)$$

which is experimentally well satisfied.

As in Section 3 we have to specify a form of a *time-independent* solution. We take here the simplest possible generalization of the SU(2) Ansatz $\overline{U}_0$ of Eq. (3.6), namely:

$$U_0 = \begin{bmatrix} & \overline{U_0} & 0 \\ & & 0 \\ 0 & 0 & 1 \end{bmatrix}. \quad (4.6)$$

The energy of the solution (4.6) is given by:

$$M = M_{\rm cl}[P] + m_{\rm cl}[P], \quad (4.7)$$

where

$$M_{\rm cl}[P] = 4\pi\frac{F_\pi}{e}\int_0^\infty dx\left(\left(\frac{x^2}{8}\frac{dP}{dx}^2 + \frac{\sin^2 P}{4}\right) + \left(\frac{\sin^4 P}{2x^2} + \frac{dP}{dx}^2\right)\right), \quad (4.8)$$

$$m_{\rm cl}[P] = \pi\frac{\mu^2}{e^3F_\pi}\int_0^\infty dx\,x^2(1 - \cos P), \quad (4.9)$$

with

$$\mu^2 = \frac{m_\pi^2 + 2m_K^2}{3} \approx (412\text{MeV})^2, \tag{4.10}$$

where $x = eF_\pi r$.

The SU(2) limit [98, 121] of the mass formula (4.7–4.9) can be taken by substituting $m_K = m_\pi$ in Eq. (4.10). The first bracket in Eq. (4.8) comes from the kinetic term of L_{Sk} (first term of Eq. (4.1), whereas the second one comes from the Skyrme term.

Now, in order to find the energy M, one should construct equation of motion and solve it, finding the profile function $P(x)$. Here we will adopt a variational approach, choosing $P = P(x/x_0)$ as in Eq. (3.7) and minimize the energy M with respect to x_0. The advantage of Ansatz (3.7) is that all integrals over dx can be performed analytically:

$$M_{cl} = \frac{F_\pi}{e}\pi^2 \frac{3\sqrt{2}}{16}\left(4x_0 + \frac{15}{x_0}\right), \tag{4.11}$$

$$m_{cl} = \frac{\mu^2}{e^3 F_\pi}\pi^2 \frac{\sqrt{2}}{2} x_0^3. \tag{4.12}$$

Minimizing Eq. (4.11) with respect to x_0 we find $x_0 = \sqrt{15/4}$, and the soliton mass $M_{cl} = 1370$ MeV, well above the nucleon mass. We will come back to the question of phenomenology in Section 4.3.

4.2. Quantizing the Skyrmion

The global symmetry of the energy for the static solution U_0 which leaves vacuum (*i.e.* $U_0(x = \infty) = \mathbf{1}$) invariant, is given by:

$$U_0 \to A U_0 A^\dagger, \tag{4.13}$$

where $A \in \text{SU(3)/U(1)}$, since $[\lambda_8, U_0] = 0$. Therefore matrix A is defined up to a *local* U(1) factor $h = \exp(i\lambda_8\phi)$, *i.e.* A and Ah are equivalent.

By promoting A to a *time-dependent* rotation $A(t)$ we introduce 8 collective coordinates [1, 106]:

$$A^\dagger(t)\frac{dA(t)}{dt} = \frac{i}{2}\sum_{\alpha=1}^{8} \lambda_\alpha \frac{da_\alpha(t)}{dt}; \tag{4.14}$$

however only first seven coordinates have a dynamical meaning. The *time-dependent* Ansatz

$$U(\vec{r}, t) = A(t) U_0(\vec{r}) A^\dagger(t) \tag{4.15}$$

leads to the following Lagrangian [1, 2]:

$$L_{\rm Sk} = -M[P] + \frac{I_A[P]}{2}\sum_{i=1}^{3}\frac{da_i}{dt}^2 + \frac{I_B[P]}{2}\sum_{k=4}^{7}\frac{da_k}{dt}^2 + \frac{N_c}{2\sqrt{3}}\frac{da_8}{dt} + \Delta m[A,P]. \quad (4.16)$$

Let us for the moment forget about the SU(3) breaking piece $\Delta m[A,P]$ equal to the second term in Eq. (4.3). In what follows we will assume that $\Delta m[A,P]$ can be treated as a perturbation, so first let us discuss the quantization of the unperturbed SU(3) symmetric system.

Lagrangian (4.16) resembles the well known quantum mechanical Lagrangian of a symmetric top [106, 11] with two moments of inertia:

$$I_A[P] = \frac{2\pi}{3e^3F_\pi}\int_0^\infty dx\,\left(x^2 + 4\left(\sin^2 P + x^2\frac{dP}{dx}^2\right)\right) \quad (4.17)$$

$$I_B[P] = \frac{\pi}{e^3F_\pi}\int_0^\infty dx\,\sin^2\frac{P}{2}\left(x^2 + \left(2\sin^2 P + x^2\frac{dP}{dx}^2\right)\right). \quad (4.18)$$

Again, two pieces originating from the kinetic part and the Skyrme term of Lagrangian (4.1) are separately displayed. Note that the two moments of inertia correspond to two different kinds of motion: I_A corresponds to the motion in the *non-strange* directions, whereas I_B is relevant for the rotations in the *strange* part of the configuration space, except for the eight direction. The term linear in $\dot{a}_8$ comes from the Wess-Zumino term of the Lagrangian (4.1).

In order to pursue the analogy with the symmetric top [11] let us identify the symmetries of the Lagrangian (4.16) without the SU(3) breaking term. There are two symmetry groups which leave $L_{\rm Sk}$ invariant:

$$\begin{aligned} A(t) &\to g_{\rm L}A(t), \qquad g_{\rm L}\in {\rm SU(3)_L},\\ A(t) &\to A(t)g_{\rm R}^\dagger, \quad g_{\rm R}\in {\rm SU(2)_R}\times {\rm U(1)_{local}}. \end{aligned} \quad (4.19)$$

Since A belongs to the coset space SU(3)/U(1) rather than to SU(3), the *right* symmetry splits into the product of $\rm SU(2)_R$ and $\rm U(1)_{local}$. *Left* SU(3) symmetry corresponds to flavor, *right* SU(2) to spin and local *right* U(1) factor results in the constraint [59-61]:

$$Y_{\rm R} = \frac{N_c}{3}, \quad (4.20)$$

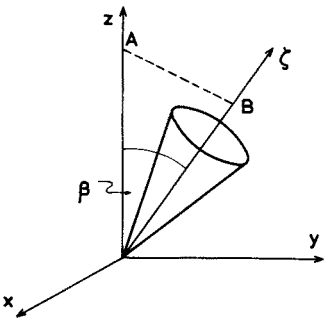

Fig. 9. Symmetric top

where Y_R is a hypercharge corresponding to the *right* U(1).

A symmetric top can be quantized by realizing that there are two sets of angular momentum operators in the problem. The three of them ($\mathbf{J}_R$) are connected with a body fixed frame (ξ, η, ζ), three others ($\mathbf{J}_L$) are defined in the LAB system (x, y, z) (see Fig. 9).

Since $[J_{\zeta,R}, J_{z,L}] = 0$, simultaneously commuting operators are: $\mathbf{J}^2 = \mathbf{J}_R^2 = \mathbf{J}_L^2, J_{z,L}$ and $J_{\zeta,R}$ corresponding to the quantum numbers j, m and k.

The wave function of the top is just a D function :

$$\begin{aligned}\psi_{top}(A) &= \sqrt{\dim(j)}D^{(j)}_{mk}(\alpha,\beta,\gamma)\\ &= \sqrt{\dim(j)}\langle (j), m \mid A(\alpha,\beta,\gamma) \mid (j), k\rangle,\end{aligned}$$

where A is an SU(2) matrix parameterized by 3 Euler angles describing the position of the top. We have consciously denoted this matrix by A since it plays exactly the same role as matrix (4.14) in the case of the Skyrme model, except that it depends on 3 instead of 7 Euler angles. Now the Hamiltonian of the symmetric top

$$\begin{aligned}H_{top} &= \frac{k^2}{2I_A} + \frac{j(j+1)-k^2}{2I_B}\\ &= \frac{C_2(\mathrm{U}(1)_R)}{2I_A} + \frac{C_2(\mathrm{SU}(2)_L) - C_2(\mathrm{U}(1)_R)}{2I_B}\end{aligned}$$

(with *left* and *right* symmetry groups defined in analogy with Eq. (4.13)) can be simply recast into the SU(3) form:

$$H^0_{Sk} = M + H_{SU(2)} + H_{SU(3)}, \tag{4.21}$$

with

$$H_{SU(2)} = \frac{C_2(\mathrm{SU(R)}_R)}{2I_A}, \tag{4.22}$$

$$H_{\mathrm{SU(3)}} = \frac{C_2(\mathrm{SU(3)_L}) - C_2(\mathrm{SU(2)_R}) - \frac{N_c^2}{12}}{2I_B}. \tag{4.23}$$

In Eq. (4.23) we have subtracted the value of the eight SU(3) generator squared from the SU(3) Casimir operator $C_2(\mathrm{SU(3)_L})$ in accordance with the constraint (4.20).

The wave function of the baryon state can be written as an SU(3) rotation matrix [122, 123]:

$$\begin{aligned}\psi_{\mathrm{baryon}}(A) &= \sqrt{\dim(p,q)}D^{(p,q)}_{mk}(A) \\ &= \sqrt{\dim(p,q)}\langle (p,q), Y, I, I_3 \mid A \mid (p,q), Y_{\mathrm{R}}, J, -J_3\rangle, \end{aligned} \tag{4.24}$$

where quantum numbers m and k denote now hypercharge, isospin and its third component, and right hypercharge, spin and its third component (with minus sign), respectively. SU(3) representations are labeled by (p, q), however not all p and q are allowed. The constraint (4.20) selects the representations of triality zero:

$$8,\ 10,\ \overline{10},\ 27,\ 35,\ \overline{35},\ 64,\ \ldots \tag{4.25}$$

for $N_c = 3$. The success of the model is the prediction that the lowest baryonic states belong to the octet and decuplet representations of SU(3). Higher representations are not predicted by the quark model but here they exist (*e.g.* the lowest $\overline{10}$ state has mass of the order of 1530 MeV).

Now we shall supplement the Hamiltonian (4.21) by the symmetry breaking term related to $\Delta m[A, P]$

$$H_{\mathrm{br}} = -\pi\frac{\Delta\mu^2}{e^3F_\pi}\langle (1,1),0,0,0 \mid A \mid (1,1),0,0,0\rangle \int_0^\infty dx\, x^2(1-\cos P), \tag{4.26}$$

with

$$\Delta\mu^2 = \frac{2}{3}(m_{\mathrm{K}}^2 - m_\pi^2) \approx (388\mathrm{MeV})^2. \tag{4.27}$$

For small $\Delta\mu^2$ the energy splittings are proportional to the averages of H_{br} between the baryonic states (B $\mid H_{\mathrm{br}} \mid$ B). These averages are given in terms of SU(3) Clebsch-Gordan coefficients [124, 125] d_{B} (see Table I and Refs [107, 2]).

Finally let us evaluate all functionals of the profile function P in terms of the Ansatz (3, 7):

$$I_A = \frac{1}{e^3F_\pi}\pi^2\frac{\sqrt{2}}{12}(6x_0^3 + 25x_0), \tag{4.28}$$

$$I_B = \frac{1}{e^3F_\pi}\pi^2\frac{\sqrt{2}}{16}(4x_0^3 + 9x_0), \tag{4.29}$$

$$H_{\mathrm{br}} = -\frac{\Delta\mu^2}{e^3F_\pi}\pi^2\frac{\sqrt{2}}{2}x_0^3 d_{\mathrm{B}}. \tag{4.30}$$

In this way we have derived the mass formula for the baryon B:

$$M_B = M_{cl} + m_{cl} + H_{SU(2)} + H_{SU(3)} + H_{br}. \tag{4.31}$$

Here all terms in Eq. (4.31) are functions of the soliton size x_0; they also depend on parameters of the meson Lagrangian, *i.e.* F_π and e. It is interesting to look at the N_c dependence [61, 66, 67] of various terms in Eq. (4.31): M_{cl}, m_{cl} and H_{br} behave explicitly as N_c. $H_{SU(2)}$ behaves as N_c^{-1} and $H_{SU(3)}$ behaves like N_c^0. Let us note that $H_{SU(3)}$ has exactly the same value between octet and decuplet states, so in practice it acts as a common mass term which shifts the classical mass of the soliton by the same amount for any physical hadronic state. Apart from the explicit N_c dependence of various terms in (4.31) there is an implicit dependence [5, 111, 112] caused by the fact, that physical baryonic states are no longer members of the octet and decuplet for $N_c \to \infty$. We will come back to this question in Section 4.5.

Note also that m_{cl} and H_{br} depend on meson masses: m_{cl} results from the explicit chiral symmetry breaking, whereas H_{br} is proportional to the SU(3) breaking parameter $m_K - m_\pi$.

In Fig.10(a) we plot M_{cl} as a function of x_0 (solid line) for a typical values of $F_\pi = 100$ MeV and $e = 5$. $M_{cl}(x_0)$ exhibits a shallow minimum; linear increase for large x_0 comes from the kinetic term whereas the rapid rise for small x_0 is due to the Skyrme term. In this sense the Skyrme term provides a hard core, preventing a soliton from shrinking to zero size. The short-dashed line represents $m_{cl}(x_0)$ — we see the rapid x_0^3 increase and long-dashed line represents $H_{SU(3)}$ (Eq. (4.23)). In the next Figure 10.b we plot M_{cl} and also $M_{cl} + m_{cl}$ (long dash), $M_{cl} + H_{SU(3)}$ (short dash) and $M_{cl} + m_{cl} + H_{SU(3)}$ (dotted line) as functions of x_0. All of them except of $M_{cl} + H_{SU(3)}$ exhibit minima however at different values of x_0 and of different magnitude. Since there is no unique prescription which combination should be actually minimized we will discuss various types of fits in the next Section.

Let us finish this Section by discussing the applicability of Ansatz (3.7) as the solution of the equation of motion obtained by minimizing the SU(3) symmetric Hamiltonian (4.21) with respect to P. Asymptotically, for large x the profile function $P(x)$ behaves as:

$$P(x) \sim \frac{1}{x^2}\Big(1 + \frac{\mu}{eF_\pi} x \exp(-\omega x)\Big), \tag{4.32}$$

where

$$\omega = \frac{1}{eF_\pi}\sqrt{\mu^2 - 2\mu_A^2 - \mu_B^2} \tag{4.33}$$

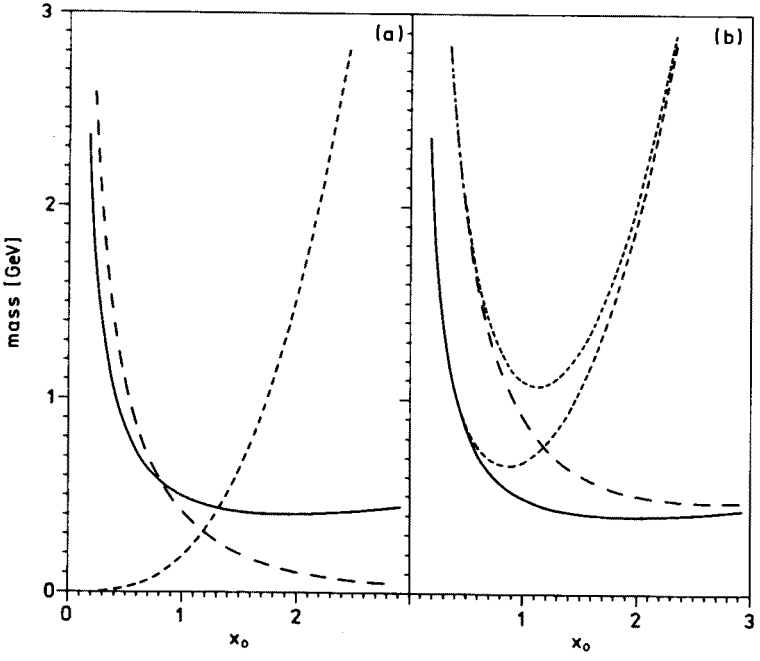

Fig. 10. Various components of the SU(3) mass formula (4.31) as functions of variational parameter x_0 for $F_\pi = 50$ MeV and $e = 5$; solid line: $M_{\rm cl}$, (a) long dash: $H_{\rm SU(3)}$, short dash: $m_{\rm cl}$; long dash: $M_{\rm cl} + H_{\rm SU(3)}$, short dash: $M_{\rm cl} + m_{\rm cl}$, dotted line: $M_{\rm cl} + m_{\rm cl} + H_{\rm SU(3)}$

with

$$\mu_A^2 = \frac{2C_2(\mathrm{SU}(2)_\mathrm{R})}{3I_A^2}, \tag{4.34}$$

$$\mu_B^2 = \frac{C_2(\mathrm{SU}(3)_\mathrm{L}) - C_2(\mathrm{SU}(2)_\mathrm{R}) - \frac{N_c^2}{12}}{4I_B^2}. \tag{4.35}$$

In the chiral limit ($\mu = 0$) $P(x) \sim x^{-2}$; Ansatz (3.7) has exactly the same behaviour. On the other hand for $\mu \neq 0$ $P(x)$ falls off much faster than Ansatz (3.7). Therefore we would expect that the results of our variational approach would be less accurate for $\mu \neq 0$. As we shall see in Section 4.3 the difference between the exact solution and the variational approach is, for most quantities, less than a few percent, implying that the shape of the tail of $P(x)$ is not very important.

Equations (4.32, 4.33) reveal another type of instability of the rotating

soliton. If $\mu^2 < \mu_A^2 - \mu_B^2$, then P starts to oscillate and the soliton decays emitting pions.

4.3. Phenomenology

Let us now discuss the relevance of the whole picture to Nature, i.e. model predictions for various physical quantities. What kind of agreement can we actually expect ? The model is in fact very simple: the starting-point Lagrangian (4.1) is the simplest one can think of, with hedgehog configuration and with Ansatz (3.7) all integrals for the mass formula and for other quantities can be performed analytically. The physical picture is also extremely simple: baryons emerge as a rigidly rotating symmetric top of the topologically nontrivial configuration of the classical pion field, chiral symmetry breaking and SU(3) breaking being treated perturbatively. All other degrees of freedom like *e.g.* vector mesons [71] are completely neglected. With this simplicity in mind it becomes clear that our predictions will be only qualitative. Still, there is a chance to gain some insight into the mechanism of chiral and SU(3) symmetry breaking, to see the importance of various terms and to find a way to generalize this oversimplified picture.

Let us now examine the mass formula (4.31). In principle one should take experimental values for F_π and e, and and obtain in this way the absolute predictions for baryon masses. This (let us call it *orthodox*) procedure, however, as discussed at the end of Section 4.1, overshoots the experimental values. Therefore Witten *et al.* [98] proposed to fit F_π and e to two baryon masses and calculate other quantities in terms of fitted model parameters (we call it a *flexible-orthodox* approach). In the most *flexible* approach one rewrites the mass formula (4.31):

$$M_B = M_1 + M_2 C_2(\mathrm{SU}(2)_R) - M_3\, d_B \tag{4.36}$$

in terms of three free parameters $M_{1,2,3}$. Here M_1 includes M_{cl}, m_{cl} and I_B, M_2 is related to I_A and M_3 contains $\widetilde{m} \to \Delta\mu^2$. Taking [11]

$$M_1 = 1144\ \mathrm{MeV}, \quad M_2 = 97\ \mathrm{MeV}, \quad M_3 = 700\ \mathrm{MeV}$$

one obtains relatively good fit to the octet and decuplet masses. The results are presented in Table I in column *A*.

It is interesting to examine the second order of the perturbative expansion. Hamiltonian H_{br} mixes octet or decuplet states with higher, unphysical representations (like *e.g.* 27, see Fig. 11). For these representations $C_2(\mathrm{SU}(3)_L) - C_2(\mathrm{SU}(2)_R) - N_c^2/12$ is different than in the case of 8 and 10;

TABLE I

Baryon masses for various fits (d_B denote group theoretical coefficients described in the text).

	d_B	exp.	A	B	C	D	E	F	[114]	[118]
N	$\frac{3}{10}$	939	941	932	1019	1083	1094	1066	1068	inp.
Λ	$\frac{1}{10}$	1116	1081	1090	inp.	inp.	inp.	inp.	1180	1046
Σ	$-\frac{1}{10}$	1193	1221	1212	1212	1147	1138	1166	1260	1120
Ξ	$-\frac{1}{5}$	1318	1291	1321	1261	1164	1149	1191	1338	1199
Δ	$\frac{1}{8}$	1232	1295	1229	1324	1365	1371	1354	1266	inp.
Σ^*	0	1385	1382	1391	inp.	inp.	inp.	inp.	1344	1302
Ξ^*	$-\frac{1}{8}$	1533	1470	1536	1446	1405	1399	1416	1435	1381
Ω	$-\frac{1}{4}$	1672	1557	1662	1506	1425	1412	1448	1521	1467
F_π		186	–	–	80	74	41	52	89	129

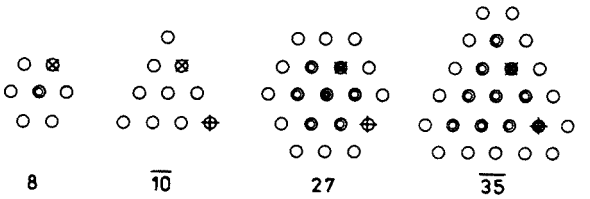

Fig. 11. States belonging to higher SU(3) representations which are mixed with proton (×) by the hamiltonian H_{br}. The same for Δ^{--} (+) if looked at upside-down

therefore the term with I_B cannot be included in M_1 any longer introducing the new, 4-th parameter M_1'':

$$M_1 = M_1' + M_1''(C_2(\mathrm{SU}(3)_\mathrm{L}) - C_2(\mathrm{SU}(2)_\mathrm{R}) - N_c^2/12).$$

Taking [11]

$$M_1' = 900\ \mathrm{MeV} \quad \text{and} \quad M_1'' = 163\ \mathrm{MeV}$$

we obtain a very good fit (see Table I, column B). There is a substantial improvement with respect to the first order formula (22). This is not a surprise since we have fitted 8 masses with 4 free parameters. Similar agreement was also obtained in Ref. [107] where an extra term $\mathrm{Tr}\,(\lambda_8 A^\dagger \dot{A})$ was added. Since this term was not present in a meson Lagrangian, its coupling was a free parameter and the total number of free parameters was

also 4. Therefore the success of fit of Ref. [107] is due the number of free parameters rather than to a physical importance of the new term.

Let us remark here that the model predicts existence of exotic states belonging to $\overline{10}$, 27 and higher representations of SU(3). For example the lightest $\overline{10}$ state of spin 1/2 and strangeness +1 has a mass of the order of 1530 MeV. It is of course an important theoretical question, which we have no answer to, whether our low energy effective theory can be applied to describe such excited states.

Columns C — F in Table I present various fits in, what we called, *flexible-orthodox* approach. Fitting procedure consisted in finding F_π and e which fit Λ and Σ^* masses. Soliton size x_0 was found by minimizing certain combination of various pieces in mass formula (4.31).

Fit C

Here we take a point of view that only $M_{\rm cl}$ is minimized treating both $m_{\rm cl}$ and $H_{\rm br}$ as perturbations. Moreover we further assume that $H_{\rm SU(3)}$ should be discarded from the mass formula since it is a *non-leading* in N_c contribution to mean octet and decuplet masses. The Skyrme Lagrangian (4.1) could be in principle enlarged by terms of the order $(1/N_c)^0$ and higher, which would also contribute to the mean octet and decuplet masses. For consistency of the N_c expansion we therefore disregard $H_{\rm SU(3)}$:

$$\begin{aligned} \text{mass} &= \overbrace{M_{\rm cl}} + m_{\rm cl} + H_{\rm SU(2)} + H_{\rm br}, \\ 1019 &= 562 + 547 + \quad 55 \quad - 145, \end{aligned}$$

where the brace indicates which part of the mass formula was minimized, and the figures below correspond to the nucleon mass (in MeV). The quantum SU(3) piece, omitted in this fit is $H_{\rm SU(3)} = 291$ MeV. The resulting F_π is given in Table I and $e = 5.8$.

Fit C' (not displayed in Table I)

takes the model mass formula at face value with $H_{\rm SU(3)}$ included:

$$\begin{aligned} \text{mass} &= \overbrace{M_{\rm cl}} + m_{\rm cl} + H_{\rm SU(2)} + H_{\rm SU(3)} + H_{\rm br} \\ 1119 &= 271 + 547 + \quad 55 \quad + \quad 291 \quad - 145. \end{aligned}$$

Again, the figures above correspond to the nucleon mass. The results for baryon masses are identical with *fit C*, the only difference being $F_\pi = 47$ MeV and $e = 7$.

Fit D

Here again we neglect $H_{\rm SU(3)}$, however we minimize both contributions to classical mass:

$$\begin{aligned} \text{mass} &= \overbrace{M_{\rm cl} + m_{\rm cl}} + H_{\rm SU(2)} + H_{\rm br}, \\ 1083 &= 888 + 180 + \quad 63 \quad - 48. \end{aligned}$$

The resulting e is 4.3 and $H_{SU(3)} = 407$ MeV.

Fit E
Again we take the model mass formula at face value with $H_{SU(3)}$ included, and minimize $M_{cl} + m_{cl}$ as in case D:

$$\begin{aligned} \text{mass} &= \overbrace{M_{cl} + m_{cl}} + H_{SU(2)} + H_{SU(3)} + H_{br}, \\ 1094 &= 507 + 123 + \quad 65 \quad + \quad 432 \quad - \quad 33. \end{aligned}$$

This is actually the procedure adopted in Ref.[2], where the soliton profile was found by solving numerically the equation of motion. The variational approach is here quite close to the exact result with $F_\pi = 41$ MeV (46 MeV in exact approach) and $e = 4.8$ (4.6).

Fit F
Here in addition we minimize $H_{SU(3)}$:

$$\begin{aligned} \text{mass} &= \overbrace{M_{cl} + m_{cl} + H_{SU(3)}} + H_{SU(2)} + H_{br}, \\ 1066 &= \quad 441 + 282 + 367 \quad + \quad 61 \quad - \quad 75. \end{aligned}$$

We have checked that the stability condition $\mu^2 < \mu_A^2 - \mu_B^2$ (see Eq. (4.32)) is not violated. Here $e = 5.4$.

Let us summarize the results of Table I. Column A, where we have used a general 3 parameter mass formula (4.36), represents the best fit one can possibly obtain with Eq. (4.31). The closest to this *ideal* is the fit of column C where the SU(3) quantum part of the hamiltonian (4.31) was neglected. However F_π needed in this fit deviates from the experimental value by more than 50 %. All other fits are worse and require even lower values of F_π. Let us mention that neglecting the common mass term m_{cl} (for which we see no reason) as well as $H_{SU(3)}$ would give the masses as in column C, but with $F_\pi = 134$ MeV. This is exactly the chiral SU(2) result of Ref. [98]. The latter might indicate that presumably one should either include higher orders in the perturbation series (like in column B) or find some other Ansatz which from the beginning breaks down the SU(3) symmetry. In fact both these approaches were examined and the results are presented in the last two columns of Table I. We shall comment more on that in Section 4.6.

Let us also mention that if the breaking terms in Eq.(4.4) are neglected (*i.e.* $m_\pi = m_K = 0$, one can fit the mean octet and decuplet masses (1151 MeV and 1385 MeV respectively) with $F_\pi = 105$ and $e = 5.4$ [1].

Technically we can understand why the fits are not satisfactory. We need to satisfy two conditions: we need relatively small common soliton

mass and rather large splittings within the multiplets. One should however remember that a too small classical mass is inconsistent with the physical picture of a slowly rotating heavy, classical object. Since splittings are proportional to x_0^3 we would like to have large x_0 which minimizes the soliton mass. As seen from Fig. 10 $M_{\rm cl}$ has a minimum at large x_0 – this corresponds to fit C. However we have still to add $m_{\rm cl}$ and also $H_{\rm SU(3)}$ which substantially increase the baryon mass.

On the other hand, if we minimize all representation-independent terms contributing to the baryon mass then x_0 is rather small (see Fig. 10) and therefore the mass splittings are not satisfactory.

In fits C', E and F the contribution of $H_{\rm SU(3)}$ and/or $m_{\rm cl}$ is relatively large (like in the fit C', where $m_{\rm cl} + H_{\rm SU(3)} \approx 3/4 M_{\rm N}$). Those fits should be discarded, since they contradict the picture of a heavy, slowly rotating classical object, whose mass is dominated by the classical part $M_{\rm cl}$ with $H_{\rm SU(3)}$ and $m_{\rm cl}$ being only a small correction.

4.4. Dilambda in the Skyrme Model

In this Section we calculate the mass of the H particle within the framework of the Skyrme model. We use exactly the same Ansatz $U_{\rm H}$ as in Eq. (3.23). The topological charge of Ansatz (3.23) is given by [56, 57]:

$$B_{\rm H} = 2\pi f(0) \tag{4.37}$$

and is independent of g. Here an important remark concerning the parity of the H particle is in order. Ansatz (3.23) has no definite behavior under the parity transformation:

$$U_{\rm H}(\vec{r}) \to U_{\rm H}^{\dagger}(-\vec{r}) \neq \pm U_{\rm H}(\vec{r}). \tag{4.38}$$

The parity transformation corresponds to a replacement $g \to -g$. Therefore, classically, the parity P $= +1$ and P $= -1$ states are degenerate in the Skyrme model. Moreover, $1/N_{\rm c}$ corrections do not lift this degeneracy. However, since two Ansätze $U_{\rm H}^{(1,2)}$ (corresponding to $g_1 = g$ and $g_2 = -g$ respectively) have the same topological number $B_{\rm H}$ (see Eq. (4.37)), there should exist a family of interpolating Ansätze $U_{\rm H}^{\rm int}(\tau)$, where $\tau \in (-\infty, \infty)$, such that [7]:

$$U_{\rm H}^{\rm int}(-\infty) = U_{\rm H}^{(1)} \quad \text{and} \quad U_{\rm H}^{\rm int}(\infty) = U_{\rm H}^{(2)}. \tag{4.39}$$

One could in principle calculate the action corresponding to the transition from $U_{\rm H}^{(1)} \to U_{\rm H}^{(2)}$ and, in this way, estimate the splitting of P $= +1$ and P $= -1$ states. In any case this splitting will be parametrically small, *i.e.* of the order $\exp(-N_{\rm c})$.

There should also exist a continuous tunnelling trajectory from H to $\Lambda\Lambda$ system which, however, can be expected to suppress $H \to \Lambda\Lambda$ decay (even if $M_H > 2M_\Lambda$) due to the fact that the pseudoscalar field configuration (3.23, 3.24) is very different from the product Ansatz of two *hedgehogs* corresponding to $\Lambda\Lambda$ configuration.

Inserting U_H into the Skyrme Lagrangian (4.1) we get the mass formula which depends on 2 trial functions f and g:

$$M_{cl}[f,g] = 2\pi \frac{F_\pi}{e} \int_0^\infty dx \left(\left(1 - \cos f \cos g + \frac{x^2}{4}\frac{\partial f}{\partial x}^2 + \frac{x^2}{12}\frac{\partial g}{\partial x}^2\right) + \left(\frac{3}{x^2}\sin^2 f \sin^2 g + \frac{1}{x^2}(1 - \cos f \cos g)^2\right) + \left(\frac{\partial f}{\partial x}^2 + \frac{\partial g}{\partial x}^2\right)(1 - \cos f \cos g)\right), \tag{4.40}$$

$$m_{cl}[f,g] = \pi \frac{\mu^2}{2e^3 F_\pi} \int_0^\infty dx\, x^2 \left(3 - 2\cos f \cos\frac{g}{3} - \cos\frac{2g}{3}\right), \tag{4.41}$$

where x and μ^2 are defined in Sect. 4.1.

Upon rotation (4.15) the mass formula $M_{cl} + m_{cl}$ gets quantum corrections, however the mass of the lowest singlet state remains unchanged. One can analytically evaluate the integral over dx in Eq. (4.40). Introducing

$$x_0 = eF_\pi r_f \quad \text{and} \quad t = \frac{r_f}{r_g}$$

we find:

$$M_{cl} = \frac{F_\pi}{e}\pi^2 \left(I_{kin}(t) x_0 + \frac{I_{Skyr}(t)}{x_0}\right), \tag{4.42}$$

where

$$I_{kin}(t) = \frac{3}{\sqrt{2}} + \frac{1}{3t} + \frac{2}{1+t^{12}}\left(-\sqrt{2}(1+t^6) + \frac{2}{3}(-t^{11} + 2t^7 + t^3 + \frac{1}{t})\right), \tag{4.43}$$

$$I_{Skyr}(t) = \frac{50}{9t} + \frac{1}{1+t^{12}}\left(-\sqrt{2}(101 - 25t^6) + \frac{2}{3}(-5t^9 - \frac{206}{3}t^5 + 170t)\right) + \frac{8}{(1+t^{12})^2}\left(\sqrt{2}(37 - 25t^6) + \frac{2}{3}(19t^9 + 54t^5 - 70t)\right) - \frac{64}{(1+t^{12})^3}\left((3\sqrt{2}(1-t^6) + 2(t^9 + 2t^5 - 2t)\right). \tag{4.44}$$

Unfortunately $m_{\rm cl}$ can be evaluated only numerically.

$$m_{\rm cl} = \pi \frac{\mu^2}{2e^3 F_\pi} x_0^3 I_m(t), \tag{4.45}$$

however $I_m(t)$ can be well approximated by a simple analytical formula for $t > 0.3$:

$$I_m(t) \equiv \int_0^\infty dx\, x^2 \Big(3 - 2\cos f(x) \cos\frac{g(tx)}{3} - \cos\frac{2g(tx)}{3}\Big)$$
$$\approx \frac{1}{2t^3\sqrt{t}} + \frac{\pi\sqrt{5}}{\sqrt{3}}.$$

Functions $M_{\rm cl}(x_0, t)$ and $M_{\rm cl}(x_0, t) + m_{\rm cl}(x_0, t)$ exhibit minima at non-zero x_0 and t. Unlike in the ordinary baryon case, the mass of the H particle is not unreasonably large for the physical values of the model parameters, *i.e.* $F_\pi = 186$ MeV and $e = 5.5$. On the contrary, $M_{\rm H}$ turns out to be just at the threshold of the two Λ state. If we minimize $M_{\rm cl}$ only, $M_{\rm H} = 2.27$ GeV ($x_0 = 1.7$ and $t = 0.9$), whereas if we minimize $M_{\rm cl} + m_{\rm cl}$ then $M_{\rm H} = 2.23$ GeV (with $x_0 = 1.4$ and $t = 0.85$).

If we take model parameters as fitted in Section 4.3 we get $M_{\rm H}$ *always* below the two Λ threshold. The smaller is F_π the lower is the H mass: for fit D in Table I $M_{\rm H} = 1.47$ GeV, whereas for fits F and E we get $M_{\rm H} = 0.85$ GeV. In all these cases $m_{\rm cl} \approx 140 - 450$ MeV, *i.e.* it is of the order of the strange quark mass rather than of the order of $2m_{\rm s}$.

Of course the result where the six-quark state has a mass smaller than the nucleon cannot be left without any comment. We have already discussed the physical relevance of the fits to baryon masses presented in the previous Section. In fits E and F the portion of the mass distributed over the terms which should constitute only small corrections to $M_{\rm cl}$ is unreasonably large. Here this pathology shows up once again in the unreasonably small H mass. For the parameters of fit D dilambda is still strongly bound, with a mass of the order of 1.5 GeV, whereas for fit C $M_{\rm H} \approx 1.3$ GeV.

4.5. Large $N_{\rm c}$ limit

As we have mentioned earlier the Skyrme model is believed to be a large $N_{\rm c}$, low energy approximation to QCD [66, 67]. In the limit of $N_{\rm c} \to \infty$ baryons consist of an *infinite* number of quarks, and therefore are infinitely heavy . In this limit they can be equivalently described as solitons of the effective meson theory [61]. In all calculations in the previous Sections we have, however, kept $N_{\rm c} = 3$. This procedure was criticized in Ref. [111],

where the authors argued that one should organize all mass formulae and expressions for other quantities as a systematic expansion in $1/N_c$. For that very reason we neglected $H_{SU(3)}$ in fits C and D in Section 4.3. In this Section we will show how the systematic expansion in N_c can be explicitly performed.

Here we immediately encounter a problem. As explained in Section 4.2 the quantization of the Skyrme model results in the constraint of Eq. (4.20):

$$Y_R = \frac{N_c}{3}.$$

For $N_c = 3$ $Y_R = 1$ and the lowest representations allowed are 8 and 10. If, however, $N_c > 3$ then the lowest possible representations have higher dimensions. The same is true in the quark model where N_c quarks forming a baryon can no longer form octet or decuplet representation of the $SU(3)_{\text{flavor}}$ group.

For an arbitrary N_c there is a number of representations (p, q) which satisfy the constraint of Eq. (4.20):

$$(N_c, 0),\ (N_c - 2, 1),\ \cdots\ (1, \tfrac{1}{2}(N_c - 1)). \tag{4.46}$$

Which of them should we call a *generalized* octet or decuplet? There are at least three possible choices of such generalization [113]:

$$\text{“8”} = \left(1, \frac{N_c - 1}{2}\right), \qquad \text{“10”} = \left(3, \frac{N_c - 3}{2}\right), \tag{4.47}$$

$$\text{“8”} = \left(\frac{N_c - 1}{2}, \frac{N_c - 1}{2}\right), \qquad \text{“10”} = \left(\frac{N_c + 3}{2}, \frac{N_c - 3}{2}\right), \tag{4.48}$$

$$\text{“8”} = \left(\frac{N_c - 1}{2}, 1\right), \qquad \text{“10”} = (N_c, 0). \tag{4.49}$$

In each of the above choices for $N_c = 3$ “8” = 8 and “10” = 10, however for $N_c > 3$ each choice corresponds to a different set of representations which we would like to call *generalized* octet and decuplet. Of course every representation in Eqs (4.47–4.49) has more than eight or ten states, however we can distinguish a subset of eight or ten states which, according to certain criterion, “look like” the states of octet or decuplet (see Fig. 12). All other states in such representation are spurious. We will always require that the *generalized* particles have physical isospin. Other quantum numbers may have, in principle, values different than in Nature.

In choice (4.47) proton has hypercharge $Y = N_c/3$ and charge $Q = (N_c + 3)/2$; all octet states have spin 1/2 and decuplet states 3/2. In choice (4.48) we require that the *generalized* octet should form a selfadjoint representation, like the physical octet. In this choice the hypercharge of the *generalized* baryons takes physical values; this condition uniquely determines the choice for the *generalized* decuplet. However in (4.48) spin takes

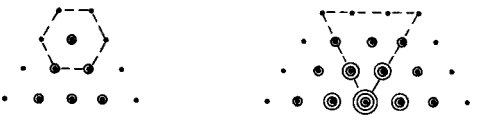

Fig. 12. SU(3) "8" and "10" representations defined in Eq. (4.47) with *octet-like* and *decuplet-like* structures

unphysical values: $(N_c - 1)/4$ and $(N_c + 3)/4$ for representations "8" and "10" respectively. In the last choice representation "10" is totally symmetric as in the case for the physical decuplet. For this choice spin as well as hypercharge are of the order of N_c.

All these choices are in principle equivalent [113]. If we however require that the soliton rotates slowly also in the large N_c limit, then only representations (4.47) are allowed, since for them spin takes always physical values. Therefore we choose (4.47) as the definitions which generalize octet and decuplet $SU(3)_{\text{flavor}}$ representations for large number of colours.

Now we can calculate the mass splittings for an arbitrary number of colors. As seen from Eq. (4.26) H_{br} is proportional to

$$\hat{\Lambda} = \langle (1,1),0,0,0 \mid A \mid (1,1),0,0,0 \rangle.$$

The coefficients d_B are defined as matrix elements of $\hat{\Lambda}$ between states of representations (4.47), and are given in terms of the $\text{SU}(3)_{\text{flavor}}$ Clebsch-Gordan coefficients. More details can be found in Appendix D; here, in Table II, we present the results [5].

For $N_c = \infty$ all d_B's are equal 1; *i.e.* $H_{\text{br}} \sim N_c$. The splittings inside each multiplet are therefore of the order of 1 except for the $\Lambda - \Sigma$ splitting which is of the order $1/N_c$. Hence we have an interesting qualitative prediction:

$$M_\Sigma - M_\Lambda < M_\Lambda - M_N, \tag{4.50}$$

$$77 \text{ MeV} < 177 \text{ MeV},$$

and

$$M_\Sigma - M_\Lambda < M_\Xi - M_\Sigma, \tag{4.51}$$

$$77 \text{ MeV} < 125 \text{ MeV},$$

which, as seen from Eqs (4.50, 4.51), agrees with the data very well. Interestingly enough, for $N_c = 3$, inequality (4.51) is reversed contradicting the experimental results. This is perhaps the most serious failure of the model [104].

TABLE II

Coefficients d_B for arbitrary N_c

B	d_B
N	$\frac{N_c^2+4N_c-3}{(N_c+3)(N_c+7)} \approx 1-\frac{6}{N_c}+\frac{36}{N_c^2}$
Λ	$\frac{N_c-2}{N_c+7} \approx 1-\frac{9}{N_c}+\frac{63}{N_c^2}$
Σ	$\frac{N_c^2+N_c-18}{(N_c+3)(N_c+7)} \approx 1-\frac{9}{N_c}+\frac{51}{N_c^2}$
Ξ	$\frac{N_c-5}{N_c+7} \approx 1-\frac{12}{N_c}+\frac{84}{N_c^2}$
Δ	$\frac{N_c^2+4N_c-15}{(N_c+1)(N_c+9)} \approx 1-\frac{6}{N_c}+\frac{44}{N_c^2}$
Σ^*	$\frac{(N_c-3)(N_c+4)}{(N_c+1)(N_c+9)} \approx 1-\frac{9}{N_c}+\frac{77}{N_c^2}$
Ξ^*	$\frac{N_c^2-2N_c-9}{(N_c+1)(N_c+9)} \approx 1-\frac{12}{N_c}+\frac{110}{N_c^2}$
Ω	$\frac{N_c^2-5N_c-6}{(N_c+1)(N_c+9)} \approx 1-\frac{15}{N_c}+\frac{143}{N_c^2}$

Can we understand inequalities (4.50) and (4.51) in terms of the quark model ? In the limit $N_c \to \infty$ nucleon has mass of the order of $N_c m_q$, where q stands for up or down quark, whereas Λ or Σ mass is of the order

$$N_c m_q + (m_s - m_q).$$

Of course the difference is of the order of 1. The $\Sigma - \Lambda$ mass difference is zero in this crude, qualitative picture, since both particles have only one strange quark. Their splitting is due to some details of the wave function and starts at the order of $1/N_c$.

Let us define new coefficients $\bar{d}_B$:

$$\bar{d}_B = 1 - d_B, \tag{4.52}$$

which are $O(1/N_c)$. We can now rewrite $m_{cl} + H_{br}$ as:

$$m_{cl} + H_{br} = \overline{m}_{cl} + \overline{H}_{br}, \tag{4.53}$$

where

$$\overline{m}_{cl} = \frac{m_\pi^2}{e^3 F_\pi} \pi^2 \frac{\sqrt{2}}{2} x_0^3 \tag{4.54}$$

is of the order of N_c, and equals to the chiral symmetry breaking term in the SU(2) case, whereas

$$\overline{H}_{\rm br} = \frac{\Delta\mu^2}{e^3 F_\pi}\pi^2 \frac{\sqrt{2}}{2} x_0^3 \bar{d}_B \tag{4.55}$$

is of the order of $O(1)$. The quality of the fits to the baryon masses is not different of those presented in Section 1.3.

4.6. Large Kaon Mass

In what we have done so far we have had explicitly assumed that $\Delta\mu^2$ is small, and subsequently, that we can treat $\overline{H}_{\rm br}$ as a perturbation. Although in various fits presented in Section 4.3 the value of the mass splitting is no larger than 150 MeV, *i.e.* 15% of the nucleon mass, it is quite plausible that the kaon mass (or $\Delta\mu^2$) is in fact too large to allow for perturbative treatment. In this Section we shall briefly report the results of two *nonperturbative* approaches.

The first one proposed by Yabu and Ando [114] consists in exactly diagonalizing $\overline{H}_{\rm br}$. In fact $\overline{H}_{\rm br}$ mixes various SU(3) representations (see Fig. 11). Here, it is useful to pursue the analogy with the symmetric top [11]. The kaon mass term acts as a spring attached to points A and B (see Fig. 9). Therefore energy is required to change the angle β, whereas $U(1)_{L,R}$ rotations with respect to axes z and ζ still correspond to the zero modes. This picture can be easily generalized to the SU(3) case. The "good" quantum numbers are isospin, hypercharge and spin; the wave function is a sum over all representations (p,q) which mix with 8 or 10. In order to calculate the elements of $\overline{H}_{\rm br}$ we have used analytical formulae for the SU(3) Clebsch–Gordan coefficients derived by methods described in Appendix D. In Fig. 4.6 we plot baryon energies calculated by diagonalizing numerically $\overline{H}_{\rm br}$ as functions of $\omega(m_K)$:

$$\omega^2 = 3I_B\pi\frac{\Delta\mu^2}{e^3F_\pi}\int dx\, x^2(1-\cos P)$$

The dashed line denoted by ϵ_0 corresponds to the energy of the state with vacuum quantum numbers. In fact $\overline{H}_{\rm br}$ mixes SU(3) singlet with the isospin singlet of the octet, 27 and higher representations of SU(3). Alternatively we can view ϵ_0 as the energy of the symmetric top which does not rotate but only oscillates in angle β. Yabu and Ando subtracted this energy from their mass formula to ensure that in the limit of $m_K \to \infty$ it reduces to the SU(2) mass formula of Eqs (4.21, 4.22). The results are presented in Table I.

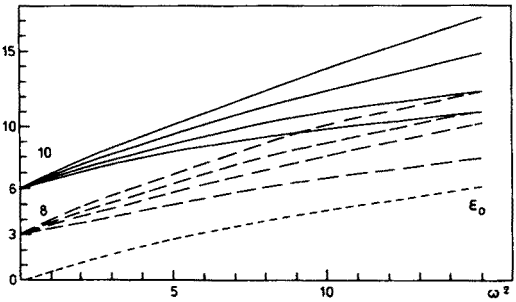

Fig. 13. Baryon masses as functions of ω in the approach of Ref.[114]

The approach of Yabu and Ando consists in fact in summing the perturbation series in m_K. This does not take into account, that for sufficiently large K mass the soliton may have tendency to deform as it deviates into the *strange* directions. Callan and Klebanov [115, 116] developed a treatment in which *strange* fluctuations about the SU(2) skyrmion are described by the following Ansatz:

$$U_{CK} = \sqrt{U_0} U_K \sqrt{U_0}, \tag{4.56}$$

where U_0 is given by Eq. (4.6) and

$$U_K = \exp\left(i \frac{2}{F_\pi} \sum_{\alpha=4}^{7} \lambda_\alpha K^\alpha \right) \tag{4.57}$$

Callan and Klebanov expand Lagrangian (4.1) up to the second order in the kaon fields K and find that a hyperon consists of a kaon bound by the SU(2) soliton. The results of the numerical analysis of Ref.[118] are presented in Table I. Although the hyperfine splittings are reproduced with good accuracy, the centroid of the hyperon spectrum is to low. In fact, the fit of Ref. [116] predicts that $m_\Xi < m_\Delta$. Let us mention that the bound-state approach has been recently used to describe charmed and bottomed baryons [118].

Both approaches described in this Section fail to explain inequality (4.51).

5. Summary

In this paper we have attempted to present the foundations of the chiral models as well as the baryon properties emerging from such models. We have selected topics discussed by the author in Refs [1–9] and in review articles [11–13]. Apart from the Skyrme model which triggered this sort of approach to the strong dynamics, we have discussed alternative quark-pion models. These models do not account for confinement. An attractive way

to incorporate confinement was developed in the chiral bag picture (see *e.g.* [15]), which, however, is plagued by infinities which have to be subtracted in an arbitrary manner.

Our goal was to present a general framework with some phenomenological applications. The material presented in this paper is by no means complete. We did not discuss in full detail the role of the Wess-Zumino term and the role of topology in chiral models, especially the fermionic nature of the soliton [62]. We have not considered vector mesons and higher excitations [71]. We have confined our discussion of phenomenology to baryon masses only, although other quantities such as magnetic moments or form-factors, have been calculated [71, 70]. Apart from static properties, dynamical characteristics, such as pion-nucleon phase-shifts [126] or weak amplitudes [3, 4], have been also discussed. Chiral models have also proven to be of value in analysis of nuclear structure [69].

Introducing strangeness to the above models creates a serious theoretical problem connected with the strange quark mass; how is m_s related to another small parameter – $1/N_c$? The approaches discussed here take two extreme points of view; m_s is very small or, to the contrary, rather large. None of them gives a really satisfactory description of the hyperon splittings. It seems that more work is needed to understand the nature of the SU(3) symmetry breaking in chiral models. The large N_c arguments presented here indicate that $1/N_c$ corrections are of importance.

We see the following points which require further study. A full analysis of hyperon mass spectrum in χQM is of course one of them. More complicated versions of the model with vector mesons also merit discussion. Finally, the interesting problem of the nucleon structure functions in deep inelastic scattering, providing an interesting link between low and high energy regimes of QCD, has not been discussed so far within the framework of χQM. From the high brow theorist's point of view, derivation of low energy action from QCD is of course a challenging problem.

This paper summarizes work done in collaboration with D.I. Diakonov, Z. Duliński, M.A. Nowak, P.O. Mazur, V.Yu. Petrov, P.V. Pobylitsa, J. Trampetić and G. Valencia whom I would like to thank for fruitful collaboration and numerous discussions. I am grateful to I.J.R. Aitchison, A. Białas, A.P. Balachandran, K. Goeke, G. Ripka, M. Rho, J. Schechter and K. Zalewski for encouragement, discussions, remarks and helpful hints. Discussions with R. Alkofer, W. Broniowski, A. Górski M. Jeżabek, M. Kutschera, and I. Zahed are gratefully acknowledged.

This work was in part supported by Polish Research Grant CPBP 01.09.

APPENDIX A
Derivative Expansion

In this Appendix we will derive the effective pion lagrangian [8] leading to coefficients α_k and β_k and to constraints (2.21) and (2.22). The effective action of Eq. (2.20) reads:

$$S_{\text{eff}}^{\text{reg}}[\pi] = -\frac{N_c}{2}\int_0^\infty \frac{dt}{t}\,\varphi(tM^2)\,e^{-tM^2}\,\text{Sp}\left(e^{t\partial^2+tMV} - e^{t\partial^2}\right), \tag{A.1}$$

where operator V is given by:

$$V = \not{\partial}\overline{U}^5. \tag{A.2}$$

Our task is now to expand Eq. (A.1) in powers of derivatives of V:

$$e^{t\partial^2+tMV} = \sum_{n=0}^{\infty}(tM)^n \int_0^1 \prod_{i=1}^{n} d\alpha_i\,\delta\left(1-\sum_{k=0}^{n+1}\alpha_k\right) S_n(\alpha_1,\alpha_2,\ldots,\alpha_{n+1}), \tag{A.3}$$

where

$$S_n(\alpha_1,\alpha_2,\ldots,\alpha_{n+1}) = \text{Sp}\left(e^{t\alpha_1\partial^2}Ve^{t\alpha_2\partial^2}V\cdots e^{t\alpha_{n+1}\partial^2}\right). \tag{A.4}$$

Next we perform functional trace introducing a complete set of normalized states $|x\rangle$:

$$S_n(\alpha_1,\alpha_2,\ldots,\alpha_{n+1}) = \text{Tr}\int\prod_{i=1}^{n} d^4x_i$$
$$\langle x_1|e^{t(\alpha_1+\alpha_{n+1})\partial^2}V|x_2\rangle\langle x_2|e^{t\alpha_2\partial^2}V|x_3\rangle\cdots\langle x_n|e^{t\alpha_n\partial^2}V|x_1\rangle, \tag{A.5}$$

where Tr denotes spinor and isospin trace. Fourier transforming $V(x)$ we find

$$\langle x_i|e^{t\beta_i\partial^2}V|x_{i+1}\rangle = \int\frac{d^4k_i}{(2\pi)^4}\frac{d^4p_i}{(2\pi)^4}e^{-ik_ix_i}\,e^{-t\beta_i(k_i+p_i)^2}\,e^{i(k_i+p_i)x_{i+1}}\,V(p_i), \tag{A.6}$$

where

$$x_{n+1}\equiv x_1,$$
$$\beta_1 = \alpha_1+\alpha_{n+1} \quad \text{and} \quad \beta_i = \alpha_i \text{ for } 1<i\le n+1.$$

After inserting Eq. (A.6) into Eq. (A.5), and introducing new variables

$$k_i \to q_i = (k_i + p_i) + i\frac{x_i - x_{i+1}}{2t\beta_i}$$

we can perform Gaussian integrals over d^4q_i:

$$\begin{aligned} S_n(\beta_1, \beta_2, \ldots, \beta_n) = &\int \prod_{i=1}^{n} d^4x_i\, \delta^4(x_1 - x_{n+1}) \prod_{i=1}^{n} \exp\left(-\frac{(x_{i+1} - x_i)^2}{4t\beta_i}\right) \\ &\int \prod_{i=1}^{n} \frac{d^4p_i}{(2\pi)^4} \exp(ip_ix_i)\, \mathrm{Tr}\,(V(p_1)V(p_2)\cdots V(p_n)) \\ &\int \prod_{i=1}^{n} \left(\frac{d^4q_i}{(2\pi)^4} \exp\left(-t\beta_i q_i^2\right)\right). \end{aligned} \tag{A.7}$$

Note that S_n does not depend on β_{n+1}. Introducing new variables:

$$x_{i+1} \to z_i = x_{i+1} - x_i, \qquad x_1 \to x$$

we get

$$\begin{aligned} S_n(\beta_1, \beta_2, \ldots, \beta_n) = &\int d^4x \int \prod_{i=1}^{n} d^4z_i\, \delta^4\left(\sum_{i=1}^{n} z_i\right) \prod_{i=1}^{n} \exp\left(-\frac{z_i^2}{4t\beta_i}\right) \\ &\int \prod_{i=1}^{n} \frac{d^4p_i}{(2\pi)^4} \exp\left(-iP_iz_i\right) \mathrm{Tr}\,(V(p_1)V(p_2)\cdots V(p_n)) \\ &\int \prod_{i=1}^{n} \left(\frac{d^4q_i}{(2\pi)^4} \exp\left(-t\beta_i q_i^2\right)\right), \end{aligned} \tag{A.8}$$

where capital P_i is defined as

$$P_i = \sum_{j=1}^{i} p_i.$$

The last step consists in Fourier transforming $\delta(\sum z_i)$ and integrating over d^4z_i. We are left with an expression containing $\mathrm{Tr}\,(V(p_1)V(p_2)\cdots V(p_n))$ and an exponent of some powers of the momenta $p_1, p_2, \ldots, p_n$, which can be rewritten in terms of an exponent of a differential operator $\mathcal{O}_n$ constructed from derivatives d/dx acting on a *given* $V(x)$ under the trace. Our final

formula reads:

$$S_{\text{eff}}^{\text{reg}}[\pi] = \frac{N_c}{32\pi^2} \sum_{n=1}^{\infty} \int_0^{\infty} \frac{dt}{t^3} (tM)^n \varphi(tM^2) \mathrm{e}^{-tM^2} \int d^4x \int_0^1 d\beta_2 \int_0^{1-\beta_2} d\beta_3 \cdots \int_0^{1-\beta_1-\beta_2-\ldots-\beta_n} d\beta_{n+1} \mathrm{e}^{t\mathcal{O}_n} \operatorname{Tr} \left(V_1(x) V_2(x) \cdots V_n(x)\right), \tag{A.9}$$

with $\beta_1 = 1 - \beta_2 - \ldots - \beta_n$. The operator $\mathcal{O}_n$ is defined as:

$$\mathcal{O}_n(\beta_1, \beta_2, \ldots, \beta_n) = \sum_{i=1}^{n} \beta_i \left(\sum_{j=1}^{i} \partial_j^{\mu} \right)^2 - \left(\sum_{i=1}^{n} \beta_i \sum_{j=1}^{i} \partial_j^{\mu} \right)^2, \tag{A.10}$$

where $\partial_j^{\mu} \equiv (\partial/\partial x_{\mu})_j$ acts only on a *given* $V_j(x)$ under the trace in Eq. (A.9). Note that $\mathcal{O}_1 = 0$ and $\mathcal{O}_2 = \beta_2(1-\beta_2)\, \partial_2 \cdot \partial_2$.

In order to compute the pion effective Lagrangian Eqs (2.3, 2.6, 2.7) let us observe that:

$$V = -i \frac{2}{F_{\pi}} \vec{\tau} \cdot \partial \vec{\pi} - \frac{2}{F_{\pi}^2} (\vec{\tau} \cdot \partial \vec{\pi}\, \vec{\tau} \cdot \vec{\pi} + \vec{\tau} \cdot \vec{\pi}\, \vec{\tau} \cdot \partial \vec{\pi}). \tag{A.11}$$

It is useful to expand (A.9) in terms of derivatives of $\overline{U}$ (in Minkowski metric):

$$\begin{aligned} S_{\text{eff}}^{\text{reg}}[\overline{U}] = {} & \frac{N_c M^2}{16\pi^2} \Phi_0 \int d^4r \operatorname{Tr} [L_{\mu} L^{\mu}] \\ & + \frac{N_c}{16\pi^2} \Phi_1 \int d^4r \operatorname{Tr} \left[(\partial_{\mu} L^{\mu})^2 + (L_{\mu} L^{\mu})^2\right] \\ & + \frac{N_c}{192\pi^2} \Phi_2 \int d^4r \operatorname{Tr} \left[L_{\mu} L_{\nu} L^{\mu} L^{\nu} - 2(L_{\mu} L^{\mu})^2\right] \\ & + O(\partial^6 \overline{U}), \end{aligned} \tag{A.12}$$

where $L_{\mu} \equiv i\overline{U}^{\dagger} \partial_{\mu} \overline{U}$. In the first order in bare quark mass matrix m we get

$$\begin{aligned} S_{m,\text{eff}}^{\text{reg}}[\overline{U}] = {} & \frac{N_c M^3}{8\pi^2} \Phi_{-1} \int d^4r \operatorname{Tr} \left[m(\overline{U}^{\dagger} + \overline{U} - 2)\right] \\ & + \frac{N_c M}{16\pi^2} \Phi_1 \int d^4r \operatorname{Tr} \left[m(\overline{U}^{\dagger} + \overline{U}) L_{\mu} L^{\mu}\right] \\ & + O(m\, \partial^4 \overline{U}). \end{aligned} \tag{A.13}$$

Let us finish by deriving the so-called *two point* or *interpolating* approximation [21] to $S_{\rm eff}^{\rm reg}[\pi]$ by cutting off the expansion (A.9) at $n = 2$. However, we will not expand $e^{\mathcal{O}_2}$. Instead, we will go back to Eq. (A.8) and keep the Fourier integral over d^4p. Introducing $\beta = \beta_2$ we get:

$$S_{\rm int}^{\rm reg}[\pi] = N_c M^2 \int \frac{d^4p}{(2\pi)^4} p^2 \,{\rm Tr}\left(\overline{U}(p)\overline{U}^\dagger(p)\right) \mathcal{G}(p^2), \tag{A.14}$$

with

$$\mathcal{G}(p^2) = \frac{1}{16\pi^2} \int_0^\infty \frac{dt}{t} \varphi(tM^2) e^{-tM^2} \int_0^1 d\beta \, e^{-t\beta(1-\beta)p^2}. \tag{A.15}$$

Trace in Eq. (A.14) extends over flavor indices only.

Formula (A.14) becomes exact in three limiting cases: *i)* low momenta: $|\partial\overline{U}| \ll M$, *ii)* high momenta $|\partial\overline{U}| \gg M$, *iii)* any momenta but small pion field, $|\log\overline{U}| \ll 1$. Comparison with the exact calculations of this paper shows that accuracy of (A.14) is not worse than 10%.

APPENDIX B
Phase Shifts

Various physical quantities related to the Dirac sea can be found from the scattering phases of the Dirac equation. In this Appendix we derive a general formula expressing functional traces through the phase shifts [49, 6]. We then give a few application of this general relation.

Let H be a Dirac Hamiltonian, *e.g.* given by Eq. (3.3), and F is some function. Suppose we want to calculate the sum over all eigenenergies:

$$\sum_n F(E_n) = {\rm Sp}\, F(H). \tag{B.1}$$

In case of a discrete spectrum the use of this formula is straightforward. In case of a continuous spectrum let us first discretize the energy levels by putting the system into a large box of radius L. The eigenenergies are then determined by the phase shifts δ_n:

$$E_n = \pm\sqrt{k_n^2 + M^2}, \quad k_n L + \delta_n = n\pi. \tag{B.2}$$

Here each level E_n corresponds to a free Hamiltonian level E_n^0 (*i.e.* $\delta_n = 0$).

We get

$$\begin{aligned}
\mathrm{Sp}\left(F(E_n) - F(E_n^0)\right) &= \sum_n \left(F(E_n) - F(E_n^0)\right) \\
&= -\frac{1}{L}\sum_n \delta_n \frac{dF}{dE_n}\frac{dE_n}{dk_n} + \sum_{\text{discrete}} \left(F(E_n) - F(E_n^0)\right) \\
&= -\int_0^\infty dk \frac{dF}{dE}\frac{dE}{dk}\frac{\delta(k)}{\pi} + \sum_{\text{discrete}} \left(F(E_n) - F(E_n^0)\right) \\
&= -\int_M^\infty dE \frac{dF}{dE}\frac{\delta(E)}{\pi} + \int_{-M}^{-\infty} dE \frac{dF}{dE}\frac{\delta(E)}{\pi} \\
&\quad + \sum_{\text{up}} \left(F(E_\lambda) - F(M)\right) + \sum_{\text{low}} \left(F(E_\lambda) - F(-M)\right).
\end{aligned} \tag{B.3}$$

In the last equation we have introduced integration over both, upper and lower continuum. We have also added to the r.h.s. of Eq. (B.3) the contribution of discrete levels if there are any. Here λ denotes all conserved quantum numbers, "up" and "low" correspond to the summation over the discrete levels which emerged from the upper or lower continuums respectively. As an application of Eq. (B.3) one can derive the Levinson theorem for the Dirac equation:

$$\delta^\lambda(M) + \delta^\lambda(-M) = n_\lambda \pi, \tag{B.4}$$

where n_λ is the number of bound states levels with given quantum numbers λ, and $\delta^\lambda(\pm M)$ are the threshold values of the phase shifts.

Let us turn back to the calculation of the nucleon mass. It has been noted in Refs [49, 6] that:

$$\mathrm{Sp}\left(H - H_0\right) = 0. \tag{B.5}$$

Putting $F(E) = E$ we find that r.h.s. of Eq. (B.3) is equal to 0. This theorem is very useful in checking the numerical calculations of the phase shifts.

The effective action given by Eq. (A.1) can be now expressed through the phase shifts. For *time-independent* Ansatz $\overline{U}$ we obtain:

$$S_{\text{eff}}^{\text{reg}}[\pi] = \frac{TN_c}{2}\,\mathrm{Sp}\left(F(H) - F(H^0)\right), \tag{B.6}$$

where

$$F(E) = \int_0^\infty \frac{dt}{\sqrt{4\pi t}\, t}\, \varphi(tM^2)\, \mathrm{e}^{-tE^2}. \tag{B.7}$$

Since the cutoff function $F(E) = F(-E)$, the effective action (B.3) can be, at least for $\varphi(tM^2)$ such that $F(E) \propto |E|$, expressed with the help of Eq. (B.5) as a sum and integral over the negative energy states only. In contrast with a *symmetric* formula (B.3) we will call such an expression *asymmetric*.

APPENDIX C
Dirac Equation with Spherical Symmetry

In this Appendix we collect formulae for spinors which diagonalize the Dirac equation (3.9). In order to get a state with a given grand-spin K we first construct two two-component spinors $\Omega^{\pm}_{(J,J_3)}$, where $\mathbf{J} = \mathbf{S} + \mathbf{L}$. The upper superscript refers to the eigenvalue L which for given J and spin $1/2$ can be either $L = J - 1/2$ or $L = J + 1/2$

$$\begin{aligned}
\Omega^{(-)}_{J,J_3} &= \frac{1}{\sqrt{2J}} \begin{bmatrix} \sqrt{J + J_3}\, Y_{J-\frac{1}{2},J_3-\frac{1}{2}} \\ \sqrt{J - J_3}\, Y_{J-\frac{1}{2},J_3+\frac{1}{2}} \end{bmatrix}, \\
\Omega^{(+)}_{J,J_3} &= \frac{1}{\sqrt{2J+2}} \begin{bmatrix} -\sqrt{J + 1 - J_3}\, Y_{J+\frac{1}{2},J_3-\frac{1}{2}} \\ \sqrt{J + 1 + J_3}\, Y_{J+\frac{1}{2},J_3+\frac{1}{2}} \end{bmatrix}.
\end{aligned} \tag{C.1}$$

Next, for the case of two flavors, we construct four four-component spinors $\Xi^{(\pm,\pm)}_{K,K_3}$. Here the second superscript, as in the case of Ω, corresponds to two ways spin and angular momentum can be coupled to form given J, and the first superscript refers to two ways J and isospin $T = 1/2$ can be coupled to form given (integer) grand-spin K

$$\begin{aligned}
\Xi^{(-,i)}_{K,K_3} &= \frac{1}{\sqrt{2K}} \begin{bmatrix} \sqrt{K + K_3}\, \Omega^{(i)}_{K-\frac{1}{2},K_3-\frac{1}{2}} \\ \sqrt{K - K_3}\, \Omega^{(i)}_{K-\frac{1}{2},K_3+\frac{1}{2}} \end{bmatrix}, \\
\Xi^{(+,i)}_{K,K_3} &= \frac{1}{\sqrt{2K+2}} \begin{bmatrix} -\sqrt{K + 1 - K_3}\, \Omega^{(i)}_{K+\frac{1}{2},K_3-\frac{1}{2}} \\ \sqrt{K + 1 + K_3}\, \Omega^{(i)}_{K+\frac{1}{2},K_3+\frac{1}{2}} \end{bmatrix}.
\end{aligned} \tag{C.2}$$

It is useful to observe that for given K and K_3:

$$
\begin{aligned}
i(\vec{n}\times\vec{\sigma})\cdot\vec{\tau}\,\Xi^{(l,j)} &= \frac{2lj}{2K+1}\left((K+\frac{1+l}{2})\Xi^{(l,-j)} - \sqrt{K(K+1)}\Xi^{(-l,j)}\right),\\
\vec{n}\cdot\vec{\tau}\,\Xi^{(l,j)} &= \frac{l}{2K+1}\left(\Xi^{(l,-j)} - l2\sqrt{K(K+1)}\Xi^{(-l,j)}\right),\\
\vec{\sigma}\cdot\vec{\tau}\,\Xi^{(l,j)} &= \frac{lj}{2k+1}\left((2K+1+l-j)\Xi^{(l,j)}\right.\\
&\qquad \left.-(l-j)^2\sqrt{K(K+1)}\Xi^{(-l,-j)}\right),\\
\vec{L}\cdot\vec{\sigma}\Xi^{(l,j)} &= -j\Big(K+\frac{1+l}{2}+j\Big)\Xi^{(l,j)},\\
\vec{n}\cdot\vec{\sigma}\Xi^{(l,j)} &= -\Xi^{(l,-j)},
\end{aligned}
\tag{C.3}
$$

where $l, j = \pm 1$, $\vec{\tau}$ denotes isospin Pauli matrices, whereas $\vec{\sigma}$ matrices are related to the spin operator, $\vec{L}$ denotes angular momentum operator (previously denoted by **L**).

With these definitions at hand we can write down the set of differential equations for functions F, G, H and J corresponding to the Dirac equation (3.9):

$$
\begin{aligned}
\frac{dF}{dr} &= \left(\frac{K}{r}+\frac{\sin P}{2K+1}\left(M+2K\,\epsilon\,\frac{\sin P}{r}\right)\right)F\\
&\quad+\left(E+M\cos P+m+\epsilon K\left(P'-K\frac{\sin 2P}{r}\right)\right)G\\
&\quad-\epsilon\,\frac{\sqrt{K(K+1)}}{2K+1}\left(2P'+\frac{\sin 2P}{r}\right)H\\
&\quad+2\sin P\,\frac{\sqrt{K(K+1)}}{2K+1}\left(M-\epsilon\,\frac{\sin P}{r}\right)J,
\end{aligned}
\tag{C.4}
$$

$$
\begin{aligned}
\frac{dG}{dr} &= \left(-\frac{K}{r}-\frac{\sin P}{2K+1}\left(M+2K\,\epsilon\,\frac{\sin P}{r}\right)\right)G\\
&\quad+\left(-E+M\cos P+m-\epsilon K\left(P'+K\frac{\sin 2P}{r}\right)\right)F\\
&\quad+\epsilon\,\frac{\sqrt{K(K+1)}}{2K+1}\left(-2P'+\frac{\sin 2P}{r}\right)J\\
&\quad+2\sin P\,\frac{\sqrt{K(K+1)}}{2K+1}\left(M-\epsilon\,\frac{\sin P}{r}\right)H,
\end{aligned}
\tag{C.5}
$$

$$\frac{dH}{dr} = \left(\frac{K+1}{r} + \frac{\sin P}{2K+1}\left(M - 2(K+1)\,\epsilon\,\frac{\sin P}{r}\right)\right) H$$
$$+ \left(E - M\cos P + m - \epsilon K\left(P' + (K+1)\frac{\sin 2P}{r}\right)\right) J$$
$$+ \epsilon\,\frac{\sqrt{K(K+1)}}{2K+1}\left(2P' - \frac{\sin 2P}{r}\right) F$$
$$+ 2\sin P\,\frac{\sqrt{K(K+1)}}{2K+1}\left(M - \epsilon\,\frac{\sin P}{r}\right) G, \tag{C.6}$$

$$\frac{dJ}{dr} = \left(-\frac{K+1}{r} - \frac{\sin P}{2K+1}\left(M - 2(K+1)\,\epsilon\,\frac{\sin P}{r}\right)\right) J$$
$$- \left(E + M\cos P + m - \epsilon K\left(P' + (K+1)\frac{\sin 2P}{r}\right)\right) H$$
$$+ \epsilon\,\frac{\sqrt{K(K+1)}}{2K+1}\left(2P' + \frac{\sin 2P}{r}\right) G$$
$$+ 2\sin P\,\frac{\sqrt{K(K+1)}}{2K+1}\left(M - \epsilon\,\frac{\sin P}{r}\right) F. \tag{C.7}$$

In the SU(3) case there are three quarks: two form isospin dublet, whereas strange quark is an isospin singlet. Therefore we have three sets of six-components flavor-spinors Σ:

$$\Sigma^{(-,i)}_{K,K_3} = N^{(-)}\begin{bmatrix} \sqrt{(K+K_3-1)(K+K_3)}\;\Omega^{(i)}_{K-\frac{1}{2},K_3-\frac{1}{2}} \\ \sqrt{2(K+K_3)(K-K_3)}\;\Omega^{(i)}_{K-\frac{1}{2},K_3} \\ \sqrt{(K-K_3-1)(K-K_3)}\;\Omega^{(i)}_{K-\frac{1}{2},K_3+\frac{1}{2}} \end{bmatrix},$$

$$\Sigma^{(0,i)}_{K,K_3} = N^{(0)}\begin{bmatrix} -\sqrt{(K+K_3)(K-K_3+1)}\;\Omega^{(i)}_{K,K_3-\frac{1}{2}} \\ \sqrt{2}\;K_3\;\Omega^{(i)}_{K,K_3} \\ \sqrt{(K-K_3)(K+K_3+1)}\Omega^{(i)}_{K,K_3+\frac{1}{2}} \end{bmatrix},$$

$$\Sigma^{(+,i)}_{K,K_3} = N^{(+)}\begin{bmatrix} \sqrt{(K-K_3+1)(K-K_3+2)}\;\Omega^{(i)}_{K+\frac{1}{2},K_3-\frac{1}{2}} \\ -\sqrt{2(K-K_3+1)(K+K_3+1)}\;\Omega^{(i)}_{K+\frac{1}{2},K_3} \\ \sqrt{(K+K_3+1)(K+K_3+2)}\;\Omega^{(i)}_{K+\frac{1}{2},K_3+\frac{1}{2}} \end{bmatrix}, \tag{C.8}$$

where normalization factors are given by:

$$N^{(-)} = \frac{1}{\sqrt{2K(2K-1)}},$$
$$N^{(0)} = \frac{1}{\sqrt{2K(K+1)}},$$
$$N^{(+)} = \frac{1}{\sqrt{(2K+2)(2K+3)}}.$$

Similarly to relations (C.3) one can derive the following identities for the SU(3) flavor-spinors:

$$\vec{n}\cdot\vec{\Lambda}\Sigma^{(l,j)} = \frac{1}{2K+1-l}\left(l\Sigma^{(l,-j)} - \frac{1}{\sqrt{2}}\sqrt{(2K+1-l)(2K+1+2l)}\Sigma^{(0,j)}\right),$$
$$\vec{n}\cdot\vec{\Lambda}\Sigma^{(0,j)} = \frac{1}{2K(K+1)}\Sigma^{(0,-j)} - \frac{\sqrt{K(2K+3)}}{2(K+1)}\Sigma^{(+,j)} - \frac{\sqrt{(K+1)(2K-1)}}{2K}\Sigma^{(-,j)},$$
$$\vec{L}\cdot\vec{\sigma}\Sigma^{(l,j)} = -j(K+\frac{1}{2}+l+j),$$
$$\vec{n}\cdot\vec{\sigma}\Sigma^{(l,j)} = -\Sigma^{(l,-j)}. \qquad (C.9)$$

APPENDIX D
Clebsch-Gordan Coefficients for Arbitrary SU(3) Representations

In this Appendix we collect our conventions for evaluating Clebsch-Gordan coefficients used in Sections 4.3 and 4.5 to calculate mass splittings [5]. In the SU(3) Skyrme model baryon wave functions (Eq. (4.24)) as well as various operators (like $H_{\rm br}$ in Eq. (4.26)) are proportional to the SU(3) D functions:

$$D^{(\rho)}_{ab}(A),$$

where subscripts a and b stand for hypercharge Y, isospin I and I_3, and superscript $\rho = (p,q)$ denotes an SU(3) representation. Matrix elements are evaluated using the formula

$$\dim(\rho_3)\int dA\,\overline{D^{(\rho_3)}_{a_3b_3}}(A)D^{(\rho_2)}_{a_2b_2}(A)D^{(\rho_1)}_{a_1b_1}(A) = \sum_\gamma \begin{pmatrix}\rho_1 & \rho_2 & \rho_3^\gamma\\ a_1 & a_2 & a_3\end{pmatrix}\begin{pmatrix}\rho_1 & \rho_2 & \rho_3^\gamma\\ b_1 & b_2 & b_3\end{pmatrix}, \qquad (D.1)$$

where symbols in large brackets denote SU(3) Clebsch–Gordan coefficients and γ is a degeneracy index described below.

Tensorial methods of calculating Clebsch–Gordan coefficients are described in Ref. [124]. Representation $\rho = (p, q)$ of SU(3) acts on a space of symmetric and traceless tensors $T^{\{q\}}_{\{p\}}$ labeled by q upper (antiquark) and p lower (quark) indices. In what follows we omit labels $\{p\}$ and $\{q\}$ and write the indices explicitly.

Let us discuss only the case when the operator transforms as an SU(3) octet. In the direct product of the octet $T^{\{1\}}_{\{1\}}$ and $T^{\{q\}}_{\{p\}}$ representation (p, q) appears twice:

$$\begin{aligned}\left(T^{i_1 i_2 \ldots i_q}_{j_1 j_2 \ldots j_p}\right)_1 &= \sum T^n_{j_1}\, T^{i_1 i_2 \ldots i_q}_{n j_2 \ldots j_p},\\ \left(T^{i_1 i_2 \ldots i_q}_{j_1 j_2 \ldots j_p}\right)_2 &= \sum T^{i_1}_n\, T^{n i_2 \ldots i_q}_{j_1 j_2 \ldots j_p},\end{aligned} \tag{D.2}$$

where the sum in (D.2) extends over all permutations of

$$\{n, \ldots, j_k, \ldots\} \quad \text{or} \quad \{n, \ldots, i_k, \ldots\}.$$

Let us distinguish the two ways in which representation $\rho = (p, q)$ was constructed introducing additional degeneracy index $\gamma = 1$ or 2, so that $\rho^{1,2}$ corresponds to the first and second line of Eq. (D.2) respectively. We define

$$\rho^{\pm} = \rho^2 \pm \alpha\, \rho^1, \tag{D.3}$$

where α is chosen in such a way that $\rho^{\pm}$ are orthogonal:

$$\alpha^2 = \frac{q(6 + 3p + 8q + 2pq + 2q^2)}{q(6 + 3q + 8q + 2qq + 2q^2)}. \tag{D.4}$$

The Clebsch–Gordan series for the highest weight of (p, q) which we denote by "p" reads:

$$\begin{aligned}\text{“p”} = N_{\pm}\Bigg(&\pm \frac{\alpha p}{\sqrt{2}}\, \Sigma^0 \otimes \text{“p”} + \frac{-2q \pm \alpha p}{\sqrt{6}}\, \Lambda \otimes \text{“p”} \mp \alpha\sqrt{p}\, \Sigma^+ \otimes \text{“n”}\\ &+ \frac{\sqrt{q}}{\sqrt{p+1}}\, \mathrm{p} \otimes \text{“}\Sigma^0\text{”} - \sqrt{q}\, \mathrm{n} \otimes \text{“}\Sigma^+\text{”}\\ &- \frac{(\pm\alpha(p+1) - q)\sqrt{p}}{\sqrt{(p+1)(p+q+1)}}\, \mathrm{p} \otimes \text{“}\Lambda\text{”}\Bigg),\end{aligned} \tag{D.5}$$

where octet operator indices are labeled by the labels corresponding to baryon octet, whereas states in the arbitrary (p, q) representation are labeled by the baryon octet states in quotation marks: "p" stands for the

highest weight; "n" has the same Y and I as "p" but I_3 smaller by 1/2; "Σ^+" has Y smaller by 1, I and I_3 greater by 1/2 than "p"; *etc.* Here

$$N_{\pm}^2 = \frac{3(p+1+q)}{2q\big(6+3p+8q+2pq+2q^2 \mp \alpha p(p+q+4)\big)}. \qquad \text{(D.6)}$$

Our phase conventions are such that the Clebsch–Gordan coefficients for $8 \otimes 8$ *i.e.* $(p = q = 1)$ agree with the standard ones [17].

$$8_{S,A} = (1,1)^{\pm}.$$

The limiting procedure for an octet requires more care since for $q = 0$ we have only one representation $(p, 0)$ in $(1,1)\otimes(p,0)$ (see Eq. (D.2)). Therefore we have:

$$10 = \frac{1}{\sqrt{2}}\left((3,0)^- - (3,0)^+\right).$$

REFERENCES

[1] P. O. Mazur, M. A. Nowak, M. Praszałowicz, *Phys. Lett.* **147B**,137 (1984).
[2] M. Praszałowicz, *Phys. Lett.* **158B**,264 (1985).
[3] M. Praszałowicz, J. Trampetić, *Phys. Lett.* **161B**, 169 (1985).
[4] M. Praszałowicz, J. Trampetić, *Fizika* **18**, 391 (1986).
[5] Z. Duliński, M. Praszałowicz, *Acta Phys. Pol.* **B18**, 1157 (1987).
[6] D.I. Diakonov, V.Yu. Petrov, M. Praszałowicz, *Nucl. Phys.* **B323**,53 (1989).
[7] D.I. Diakonov, V.Yu. Petrov, P.V. Pobylitsa, M. Praszałowicz, *Phys. Rev.* **D39**, 3509 (1989).
[8] M. Praszałowicz, G. Valencia, *Nucl. Phys.* **B341**, 27 (1990).
[9] M. Praszałowicz, *Phys. Rev.* **D42**, 216 (1990).
[10] Proceedings of the *Workshop on Skyrmions and Anomalies*, eds M. Jeżabek, M. Praszałowicz, World Scientific, 1987.
[11] M. Praszałowicz, in Proceedings of the *Workshop on Skyrmions and Anomalies*, eds M. Jeżabek, M. Praszałowicz, World Scientific, 1987, p.112.
[12] M. Praszałowicz,in Springer Proceedings in Physics 26, *The Elementary Structure of Matter*, eds N. Boccara, J.-M. Richard, E. Aslanides, Springer Verlag,1987,p.133.
[13] M. Praszałowicz, in International Symposium on Hypernuclear and Low Energy Kaon Physics, *Nuovo Cimento* **A102**, 39 (1989).
[14] *Chiral Solitons*, ed. K.-F. Liu, World Scientific, 1987.
[15] R.K. Bhaduri, *Models of the Nucleon; From Quarks to Soliton*, in Lecture Notes and Supplements in Physics, Addison-Wesley Pub. Co., Inc, 1989.
[16] E.M. Nyman, D.O. Riska, *Rep. Prog. Phys.* **53**, 1137 (1990).
[17] C.-H. Tze, in *Chiral Solitons*, ed. K.-F. Liu, World Scientific, 1987, p.1.

[18] M. Rho, *Prog. Part. and Nucl. Phys.* **11**, 379 (1984).
[19] R. Ball, *Phys. Rep.* **182**, 1 (1989).
[20] D.I. Dyakonov, V.Yu. Petrov, *Nucl. Phys.* **B272**, 457 (1986).
[21] D.I. Dyakonov, in Proceedings of *Workshop on Skyrmions and Anomalies*, eds M. Jeżabek, M. Praszałowicz, World Scientific, 1987, p. 27.
[22] I.J.R. Aitchison, in Proceedings of *Workshop on Skyrmions and Anomalies*, eds M. Jeżabek, M. Praszałowicz, World Scientific, 1987, p. 5.
[23] P. Simić, *Phys. Rev. Lett.* **55**, 40 (1985).
[24] P. Simić, *Phys. Rev.* **D34**, 1903 (1986).
[25] J. Balog, *Phys. Lett.* **149B**, 197 (1984).
[26] I.J.R. Aitchison, C.M. Fraser, E. Tudor, J. Zuk, *Phys. Lett.* **165B**, 162 (1985).
[27] N.I. Karchev, A.A. Slavnov *Teor. & Mat. Fiz.* **65**, 192 (1985).
[28] Y. Nambu, G. Jona-Lasino, *Phys. Rev.* **124**, 246 (1961).
[29] D.I. Dyakonov, V. Yu. Petrov, *Nucl. Phys.* **B245**, 259 (1984).
[30] E.V. Shuryak, *Phys. Rev.* **115**, 151 (1985).
[31] D.I. Dyakonov, A.D. Mirlin, *Phys. Lett.* **203B**, 63 (1988).
[32] I.J.R. Aitchison, C.M. Fraser, *Phys. Lett.* **146B**, 63 (1984).
[33] S. Kahana, G. Ripka, V. Soni, *Nucl. Phys.* **A415**, 351 (1984).
[34] S. Kahana, G. Ripka, V. Soni, *Nucl. Phys.* **A429**, 462 (1984).
[35] M.S. Birse, M.K. Banerjee, *Phys. Lett.* **136B**, 284 (1984).
[36] I.J.R. Aitchison, C.M. Fraser, *Phys. Rev.* **D31**, 2605 (1985).
[37] A. Dhar, R. Shankar, R.S. Wadia, *Phys. Rev.* **D31**, 3256 (1985).
[38] V. Soni, *Phys. Lett.* **183B**, 91 (1987).
[39] V. Soni, *Phys. Lett.* **195B**, 569 (1987).
[40] T.H.R. Skyrme, *Proc. R. Soc. London* **A260**, 127 (1961).
[41] T.H.R. Skyrme, *Nucl. Phys.* **31**, 556 (1962).
[42] G. Ripka, S. Kahana, *Phys. Rev.* **D36**, 1233 (1987).
[43] J. Schwinger, *Phys. Rev.* **82**, 664 (1951).
[44] A.P. Balachandran, G. Marmo, V. Nair, C. Trahern, *Phys. Rev.* **D25**, 2713 (1982).
[45] R. Nepomechie, *Ann. Phys. (N.Y.)* **158**, 67 (1984).
[46] R. Nepomechie, *Phys. Rev.* **D31**, 3291 (1985).
[47] J. Zuk, *Z. Phys.* **29**, 303 (1985).
[48] R. Ball, *Phys. Lett.* **171B**, 435 (1986).
[49] D.I. Dyakonov, V.Yu. Petrov, V. Pobylitsa, *Nucl. Phys.* **B306**, 809 (1988).
[50] H. Reinhardt, R. Wünsch, *Phys. Lett.* **215B**, 577 (1988).
[51] K. Goeke, M. Harvey, F. Grümmer, J. Urbano, *Phys. Rev.* **D37**, 754 (1988).
[52] Th. Meissner, F. Grümmer, K. Goeke, *Phys. Lett.* **227B**, 296 (1989).
[53] Th. Meissner, F. Grümmer, K. Goeke, *Ann. Phys. (N.Y.)* **202**, 297 (1990).
[54] P. Jain, R. Johnson, J. Schechter, *Phys. Rev.* **D38**, 1571 (1988).
[55] R. Alkofer, *Phys. Lett.* **236B**, 310 (1990).
[56] A.P. Balachandran *et al.*, *Phys. Rev. Lett.* **52**, 887 (1984).
[57] A.P. Balachandran *et al.*, *Nucl. Phys.* **B256**, 525 (1985).
[58] R.L. Jaffe, *Phys. Rev. Lett.* **38**, 195 (1977).

[59] P. Barnes, in Springer Proceedings in Physics 26,*The Elemntary Structure of Matter*,eds N. Boccara, J.-M. Richard, E. Aslanides, Springer Verlag, 1987, p. 292.
[60] K. Goeke, A.Z. Górski, F. Grümmer, Th. Meissner, H. Reinhardt, R. Wünsch, Quantization of the Nambu–Jona-Lasinio soliton and the nucleon-delta splitting, Bochum Univ. preprint, 1991.
[61] E. Witten, *Nucl. Phys.* **B160**, 57 (1979).
[62] E. Witten, *Nucl. Phys.* **B223**, 422 (1983).
[63] E. Witten, *Nucl. Phys.* **B223**, 433 (1983).
[64] A.P. Balachandran, V.P. Nair, S.G. Rajeev, A. Stern, *Phys. Rev. Lett.* **49**, 1124 (1982).
[65] A.P. Balachandran, V.P. Nair, S.G. Rajeev, A. Stern, *Phys. Rev.* **D27**, 1153 (1983).
[66] G. 't Hooft, *Nucl. Phys.* **B72**, 461 (1974).
[67] G. 't Hooft, *Nucl. Phys.* **B75**, 461 (1974).
[68] G.S. Adkins, in *Chiral Solitons*, ed. K.-F. Liu, World Scientific, 1987, p. 99.
[69] I. Zahed, G.E. Brown, *Phys. Rep.* **142**, 1 (1986).
[70] U.G. Meissner, I. Zahed, *Adv. Nucl. Phys.* **17**, 143 (1086).
[71] U.G. Meissner, *Phys. Rep.* **161**, 213 (1988).
[72] M. Kutschera, W. Broniowski, A. Kotlorz, *Nucl. Phys.* **A516**, 566 (1990).
[73] W. Broniowski, A. Kotlorz, M. Kutschera, *Acta Phys. Pol.* **B22**, 145 (1991).
[74] R. Ball, in *Workshop on Skyrmions and Anomalies*, eds M. Jeżabek, M. Praszałowicz, World Scientific, 1987, p. 54.
[75] A. Adrianov, *Phys. Lett.* **157B**, 425 (1985).
[76] E. Ruiz Arriola, The low energy expansion of the generalized SU(3) NJL-model, Bochum Univ. preprint, 1990, submitted to *Phys. Lett.* B.
[77] S. Weinberg, *Phys. Rev.* **166**, 1569 (1968).
[78] J. Gasser, H. Leutwyler, *Ann. Phys. (N.Y.)* **158**, 142 (1984).
[79] J. Gasser, H. Leutwyler, *Nucl. Phys.* **B250**, 465 (1985).
[80] J.F. Donoghue, C. Ramirez, G. Valencia, *Phys. Rev.* **D38**, 2195 (1988).
[81] B. Martin, D. Morgan, G. Shaw, *Pion-Pion Interactions in Particle Physics*, Academic Press, London 1976.
[82] A. Manohar, H. Georgi, *Nucl. Phys.* **B234**, 189 (1984).
[83] S. Weinberg, *Phys. Rev. Lett.* **65**, 1181 (1990).
[84] D.I. Dyakonov, V. Yu. Petrov, M. Pobylitsa, *Phys. Lett.* **205B**, 372 (1988).
[85] D.I. Dyakonov, M. Eides, *JETP Lett.* **38**, 433 (1983).
[86] J.F. Donoghue, in *Symmetric Violations in Subnuclear Physics*, eds B. Castel, P. O'Donnel, World Scientific, 1989.
[87] J. Bijnens, S. Dawson, G. Valencia, $\gamma\gamma \to \pi^0\pi^0$ and $K_L \to \pi^0\gamma\gamma$ in the chiral quark model, preprint CERN-TH-6026/91, 1991.
[88] J. Gasser, M.E. Sainio, A. Svarc, *Nucl. Phys.* **B307**, 779 (1988).
[89] J. Gasser, H. Leutwyler, M.P. Locher, M.E. Sainio, *Phys. Lett.* **213B**, 85 (1988).
[90] P.J. Mulders, A.T. Aerts, J.J. de Swart, *Phys. Rev.* **D21**, 2653 (1980).
[91] J.L. Rosner, *Phys. Rev.* **D33**, 2043 (1986).

[92] P. MacKenzie, H.B. Thacker, *Phys. Rev. Lett.* **55**, 2539 (1985).
[93] Y. Iwasaki, T. Yoshié, T. Tsubai, *Phys. Rev. Lett.* **60**, 1371 (1988).
[94] M. Oka, K. Shimizu, K. Yazaki, *Phys. Lett.* **130B**, 365 (1983)
[95] U. Straub *et al.*, *Phys. Lett.* **200B**, 241 (1988).
[96] R.L. Jaffe, C.L. Korpa, *Nucl. Phys.* **B258**, 468 (1985).
[97] S.A. Yost, C.R. Nappi, *Phys. Rev.* **D32**, 816 (1985).
[98] G.S. Adkins, C.R. Nappi, E. Witten, *Nucl. Phys.* **B228**, 552 (1983).
[99] J. Gasser, H. Leutwyler, *Phys. Rep.* **87**, 77 (1982).
[100] R. Koch, *Z. Phys.* **C15**, 161 (1982).
[101] W. Wiedner *et al.*, *Phys. Rev. Lett.* **58**, 648 (1987).
[102] J.F. Donoghue, C.R. Nappi, *Phys. Lett.* **168B**, 105 (1986).
[103] R.L. Jaffe, C.L. Korpa, *Comm. Part. Nucl. Phys.* **17**, 163 (1987).
[104] D.B. Kaplan, I. Klebanov, *Nucl. Phys.* **B335**, 45 (1990).
[105] A.P. Balachandran, Syracuse University preprint, SU-4428-361, 1987.
[106] S. Jain, S.R. Wadia, *Nucl. Phys.* **B258**, 713 (1985).
[107] E. Gaudagnini, *Nucl. Phys.* **B236**, 35 (1984).
[108] M. Chemtob, *Nucl. Phys.* **B256**, 600 (1985).
[109] E. Gaudagnini, *Phys. Lett.* **146B**, 237 (1984).
[110] G.S. Adkins, C.R. Nappi, *Nucl. Phys.* **B249**, 507 (1986).
[111] G. Karl, J. Patera, S. Peratnis, *Phys. Lett.* **172B**, 49 (1986).
[112] J. Bijnens, H. Sonoda, M.B. Wise, *Can. J. Phys.* **64**, 1 (1986).
[113] Z. Duliński, *Acta Phys. Pol.* **B19**, 891 (1988).
[114] H. Yabu, K. Ando, *Nucl. Phys.* **B301**, 601 (1985).
[116] C.G. Callan, K. Hornbostel, I. Klebanov, *Phys. Lett.* **202B**, 269 (1988).
[117] M.A. Nowak, M. Rho, N. Scoccola, *Phys. Lett.* **201B**, 425 (1988).
[118] M. Rho, D.O. Riska, N.N. Scoccola, The energy levels of the heavy flavour baryons in the topological soliton model, Niels Bohr Inst. preprint, NBI-91-03, 1991.
[119] C. Callan, C. Coleman, J. Wess, B. Zumino, *Phys. Rev.* **177**, 2247 (1969).
[120] J. Wess, B. Zumino, *Phys. Lett.* **37B**, 95 (1971).
[121] G.S. Adkins, C.R. Nappi, *Nucl. Phys.* **B233**, 109 (1984).
[122] T.J. Nelson, *J. Math. Phys.* **8**, 857 (1967).
[123] D.F. Holland, *J. Math. Phys.* **10**, 531 (1969).
[124] J.J. de Swart, *Rev. Mod. Phys.* **35**, 916 (1963).
[125] P. McNamee, S.J. Chilton, F. Chilton, *Rev. Mod. Phys.* **9**, 1005 (1964).
[126] G. Holzwarth, B. Schwesinger, *Rep. Prog. Phys.* **49**, 825 (1986).